Course 8

WAVES IN THE PRESENCE OF MAGNETIC FIELDS, ROTATION AND CONVECTION

Christopher C. Finlay

Institute for Geophysics, ETH Zurich,
Switzerland

Ph. Cardin and L.F. Cugliandolo, eds.
Les Houches, Session LXXXVIII, 2007
Dynamos


2007 8 22

Contents

Preamble

Geophysical and astrophysical bodies commonly possess self-sustained magnetic fields due to dynamo action in their fluid regions. These systems are often also rapidly-rotating and convecting. The fluid dynamics underlying the dynamo process is consequently a competition between the stabilizing influence of rotation and magnetic fields and the forcing away from equilibrium provided by convection and perhaps also precessional or tidal driving. The stability endowed by magnetic fields and rotation simultaneously provides a basis for wave motions; these are the focus here.

This chapter is designed to be a primer for students and researchers wishing for an introduction to the physics of the waves that can exist in rapidly-rotating, hydromagnetic systems. The magnetic tension waves of Alfvén, Inertial waves arising from the intrinsic stability of rotating fluids, and the Magnetic Coriolis (MC) waves arising when these phenomenon occur in concert are described. The influence of density stratification and convective instability leading to Magnetic Archimedes Coriolis (MAC) waves is reviewed and the importance of diffusive effects and spherical geometry are outlined. Connections to recent laboratory experiments, numerical dynamo simulations and geophysical and astrophysical observations are also discussed.

This written account is an extended version of a lecture given during the 'Dynamos' summer school held at Les Houches in August 2007. The organizing committee did an excellent job of charming me from my seat in the audience to the front of the lecture theatre. I thank them for that invitation and hope that this account is of use both to my fellow attendees and to future students. The basis for my lecture and this article was a review chapter from my Ph.D. thesis [43] and two articles that appeared recently in the Encyclopedia of Geomagnetism and Palaeomagnetism [44, 45].

1. Introduction

1.1. Some motivating thoughts concerning the study of waves

Laboratory experiments studying the influence of rotation and magnetic fields on electrically conducting fluids dramatically demonstrate the intrinsic stability that these influences can impart to the fluids. Some beautiful examples of such stability have been captured in National Committee for Fluid Mechanics films on Rotating Fluids [47] and Magnetohydrodynamics [92]. Excerpts from these films were shown during the summer school and they can also be found online; they vividly illustrate the fundamental phenomena involved and are strongly recommended for the physical insight they provide.

We can intuitively understand how stability might come about in magnetic and rotating fluids by considering how magnetic field lines and vorticity lines threading through fluid parcels will effectively impart elasticity to the fluid. If some disturbance, instability, or forcing then moves fluid parcels, the tension in the magnetic field lines and vortex lines will seek to return the parcels to their original position. Such reasoning leads us to expect that fluids that undergo rotation or that are electrically conducting and permeated by a magnetic field should support oscillations and waves.[1]

Waves occurring as a result of the stability imparted by fluid rotation are known as Inertial waves. They are observed in natural rotating fluid systems such as Earth's ocean. Waves in electrically conducting fluids occurring as a result of the stability imparted by magnetic fields are known as hydromagnetic or Alfvén waves. They are found in plasmas or fluids with high electrical conductivity, such as the solar corona and Earth's magnetosphere and core. It is therefore a matter of considerable geophysical and astrophysical importance to understand and be able to quantitatively model such waves and their generalizations that occur when both magnetic fields and rotation are present.[2] This is the primary motivation behind this present chapter.

One may wonder what can be gained from the study of waves. A glance at the progress made in seismology, helioseismology and oceanography provides a vivid illustration of what may be achieved. Waves properties, particularly their dispersion, and how these vary with location and time depend on the nature of the system supporting the waves. Study of waves thus allows underlying physical properties of often inaccessible geophysical and astrophysical systems to be investigated. Furthermore, waves are a mechanism by which energy and momentum can be transported; observations of waves can therefore tell us much about how the underlying system is operating and evolving.

[1] The waves discussed in this chapter fundamentally involve the momentum equation (often coupled to the induction and heat equations) and rely on restoring forces for their existence. Dynamo waves [76] which are oscillatory solutions to the induction equation are not considered here because they are a purely kinematic phenomenon involving the magnetic field alone.

[2] No account is taken here of compressibility effects and associated acoustic waves. Readers interested in systems where compressibility is important can if necessary generalize the treatment given here. They may also wish to consult the books by Lighthill [68] and Sturrock [97] for introductions to acoustic waves and their modification in the presence of magnetic fields respectively; the review by Roberts [87] gives further technical detail.

The subject of waves in the presence of rotation, magnetic fields and convection has a long and rich history. Before embarking on a detailed account of the physics of such waves, it is useful to sketch the history of investigations into these phenomena, to acknowledge the contributions of the scientists who have laboured on this subject, to collect useful references for further reading, and to introduce necessary terminology.

1.2. Historical sketch and literature survey

The first work on oscillations and waves arising from the intrinsic stability of a rotating fluid was carried out by Lord Kelvin in 1880 [58] in a cylindrical geometry. Poincaré [78], Bryan [12] and Cartan [18] later studied similar motions in rotating spheroids. Bjerknes and co-workers [8] independently re-discovered these rotation-reliant motions, naming them 'Elastoid-Inertia' oscillations. Much of the early work is collected in the monograph by Greenspan [49] where both Inertial waves in unbounded fluids and Inertial wave modes in contained geometries are described. Recently, considerable theoretical progress has been made towards finding explicit Inertial wave mode solutions in full sphere, spheroid and cylindrical geometries by Zhang and co-workers [108–110], and in spherical shells by Rieutord and co-workers [80, 81].

The basic mechanism underlying waves in electrically conducting fluids permeated by magnetic fields was elucidated by Alfvén [5]. He described a scenario whereby magnetic tension and inertial effects give rise to oscillations and travelling waves, which became known as Alfvén waves in his honour. In this account, any wave involving both magnetic field and fluid mechanical effects will be referred to a hydromagnetic wave; Alfvén waves are the simplest possible example of hydromagnetic waves.

Lehnert [66] deduced that rapid rotation of a hydromagnetic system would lead to the splitting of plane Alfvén waves into two circularly polarized, transverse, waves. He realized these would have very different timescales if the frequency of Inertial waves was much larger than that of pure Alfvén waves in the system. Here, such waves will be collectively be referred to as Magnetic Coriolis (MC) waves. Chandrasekhar [21] studied the effects of buoyancy on rotating hydromagnetic systems, though he focused primarily on axisymmetric motions. Braginsky [9, 10] described the influence of density stratification and convection driving non-axisymmetric waves naming these Magnetic Archimedes Coriolis (MAC) waves.

Hide [52] was the first to consider the influence of spherical geometry on two dimensional (being invariant parallel to the rotation axis) hydromagnetic waves in a rapidly-rotating fluid. He studied the effects of a linear variation of the Coriolis force with distance from the rotation axis, mimicking the effect of the variation in the Coriolis force with latitude in a spherical shell (known as the β effect in meteorology and oceanography). This is the essential ingredient needed for Rossby waves [77]. He found a similar mode splitting to that discovered by Lehnert; here Hide's waves arising from the magnetic modification of Rossby waves are referred to as MC Rossby waves (see Appendix A). Malkus [70] studied MC waves in a full sphere for the special case of a background magnetic field increasing in strength with distance from the rotation axis (see Appendix B). Stewartson [95] also developed an asymptotic theory of MC waves in a thin spherical shell geometry.

Eltayeb and Roberts [27, 29, 83] and more recently Roberts and Jones [55, 86] have studied MAC waves driven by thermal instability in a rotating plane layer permeated by a strong, uniform magnetic field. They demonstrated the importance of including magnetic and thermal diffusion in such systems, but nonetheless found that it is sometimes possible for thermal instability to drive diffusionless MC and MAC waves. Busse [14] and Soward [93] extended these studies to MAC waves in a quasi-geostrophic (QG) sloping annulus geometry. This involved a formally correct description of the arrangement suggested by Hide [52] for capturing the Rossby wave mechanism thought to be relevant in a thick spherical shell geometry (see Appendix C).

Acheson [1] pointed out that hydromagnetic waves could also be driven via magnetic field instability. Fearn [36–38] later studied this mechanism in more detail using numerical simulations. Roberts and Loper [85] further illustrated that magnetic field instability can excite hydromagnetic waves, even in the presence of stable stratification. An excellent discussion of the counter-intuitive means by which magnetic or thermal diffusion can facilitate instability is given by Acheson [2].

Eltayeb and Kumar [28] and Fearn [35] carried out the first numerical studies of thermally-driven hydromagnetic waves including the effects of both buoyancy and diffusion in a rapidly-rotating, full sphere geometry. Fearn and Proctor [40] and later Zhang [103, 106] went on to consider the effect of more general background magnetic field configurations. They found that if the imposed magnetic field drives a magnetic wind this can (via a Doppler shift) greatly change the observed hydromagnetic wave frequencies.

The overviews by Hide and Stewartson [53] and Braginsky [11] provide concise introductions to the theory of hydromagnetic waves in rapidly-rotating systems. The textbooks by Melchoir [73] and Davidson [22] and the lengthy review of Gubbins and Roberts [50] contain useful summaries of hydromagnetic wave theory in the context of more general surveys of the magnetohydrodynamics. A number of more focused technical reviews of the subject also exist including those by Roberts and Soward [82], Acheson and Hide [3], Eltayeb [30], Fearn Roberts and Soward [41], Proctor [79], Zhang and Schubert [107] and most recently by Soward and Dormy [94]. Finally, in the context of the role played by hydromagnetic waves in dynamo action (the central theme of the summer school!), chapter 10 of Moffatt's monograph [74] remains essential reading.

2. Inertial waves and intrinsic stability due to rotation

2.1. The Coriolis force, vortex lines and Inertial oscillations in rotating fluids

This section I begin by considering the purely hydrodynamic case of a homogeneous fluid undergoing rapid rotation, in the absence of magnetic fields and convection. Rotation imparts intrinsic stability to the fluid due to the action of the Coriolis force on fluid parcels. The Coriolis force is well known as being the origin of circulating eddies in rotating fluids, for example, in hurricanes in Earth's atmosphere. The Coriolis force occurs only in rotating reference frames where inertial motions follow curved trajectories. Acting at right angles to direction of fluid motion, the Coriolis force results in circular motions of fluid elements, so that they periodically return to their initial position after being perturbed. This is the origin of the intrinsic stability possessed by rotating fluids [7, 98].

An intuitive understanding of this stability may be gained by thinking in terms of vortex lines which point in the direction of the local vorticity [58, 67]. Vortex lines resulting from the presence of the Coriolis force are initially parallel to the rotation vector for a homogeneous fluid in solid body rotation. They act by imparting an effective elasticity to the fluid by resisting fluid motions that distort them. This resistance of vortex lines to distortion is what gives rise to Inertial oscillations and waves [67, 68]. An alternative introductory perspective on inertial waves is given by Tritton [98], while the monography by Greenspan [49] and the review article by Stewartson [96] provide more comprehensive surveys.

2.2. The Inertial wave equation

For an infinite plane layer of homogeneous fluid with density ρ undergoing rotation with angular speed Ω, considering small velocity perturbations $\boldsymbol{u}$ about a state of rest in the rotating frame the linearized momentum equation takes the form

$$\underbrace{\frac{\partial \boldsymbol{u}}{\partial t}}_{\substack{\text{Inertial}\\\text{acceleration}}} + \underbrace{2(\boldsymbol{\Omega} \times \boldsymbol{u})}_{\substack{\text{Coriolis}\\\text{acceleration}}} = \underbrace{-\frac{1}{\rho}\nabla p}_{\substack{\text{Pressure}\\\text{gradient}}}, \tag{2.1}$$

where p is the mechanical pressure of the fluid, $\boldsymbol{\Omega} = \Omega z$ and Cartesian coordinates have been used. An equation describing the waves supported by this system can be derived by taking the curl of (2.1) and which leads to an equation describing the evolution of the fluid vorticity $\boldsymbol{\xi} = \nabla \times \boldsymbol{u}$

$$\frac{\partial \boldsymbol{\xi}}{\partial t} = 2(\boldsymbol{\Omega} \cdot \nabla)\boldsymbol{u}. \tag{2.2}$$

Taking a further curl and also a time derivative and noting that $\nabla \times \boldsymbol{\xi} = -\nabla^2 \boldsymbol{u}$ for incompressible fluids yields

$$\frac{\partial^2(\nabla^2 \boldsymbol{u})}{\partial^2 t} = -2(\boldsymbol{\Omega} \cdot \nabla)\frac{\partial \boldsymbol{\xi}}{\partial t}. \tag{2.3}$$

Using (2.2) again leads to a wave equation for the perturbation of the velocity field,

$$\frac{\partial^2(\nabla^2 \boldsymbol{u})}{\partial^2 t} = -4(\boldsymbol{\Omega} \cdot \nabla)^2 \boldsymbol{u}. \tag{2.4}$$

This is the Inertial wave equation in a rotating incompressible fluid, so called because it relies only on inertia and the Coriolis force; the later is itself a consequence of inertia in a rotating reference frame.

2.3. Inertial wave dispersion relation and properties

The properties of Inertial waves can be determined using the plane wave ansatz

$$\boldsymbol{u} = \mathcal{R}e\{\widehat{\boldsymbol{u}} e^{i(\boldsymbol{k}\cdot\boldsymbol{r}-\omega t)}\}. \tag{2.5}$$

Substituting from (2.5) into (2.4) yields

$$\omega^2 |\boldsymbol{k}|^2 \widehat{\boldsymbol{u}} = -4(\boldsymbol{\Omega} \cdot \boldsymbol{k})^2 \widehat{\boldsymbol{u}}, \tag{2.6}$$

which simplifies to the classic inertial wave dispersion relation [49],

$$\omega = \pm \frac{2(\boldsymbol{\Omega} \cdot \boldsymbol{k})}{|\boldsymbol{k}|} = \pm 2\Omega \cos\theta, \tag{2.7}$$

where θ is the angle between $\boldsymbol{\Omega}$ and $\boldsymbol{k}$, so that the angular frequency of Inertial waves is restricted to lie between 0 and $\pm 2\Omega$ s^{-1}.

The phase velocity (the speed and direction in which individual peaks and troughs move) is ω/k in the direction of the wavevector $\widehat{\boldsymbol{k}}$; for Inertial waves this is

$$C_{\mathrm{ph}} = \frac{\omega(\boldsymbol{k})}{|k|}\widehat{\boldsymbol{k}} = \pm \frac{2(\boldsymbol{\Omega} \cdot \boldsymbol{k})}{|\boldsymbol{k}|^3}\boldsymbol{k}. \tag{2.8}$$

In contrast, the group velocity (the speed and direction at which energy is transferred, see the book of Lighthill [68]) is the derivative of ω with respect to $\boldsymbol{k}$,

$$C_g = \frac{\partial \omega(\boldsymbol{k})}{\partial \boldsymbol{k}} = \pm \frac{2(k^2 \boldsymbol{\Omega} - (\boldsymbol{\Omega} \cdot \boldsymbol{k})\boldsymbol{k}}{|\boldsymbol{k}|^3}. \tag{2.9}$$

An interesting consequence of this expression for the group velocity is that when the frequency of inertial waves is very small (i.e. $(\boldsymbol{\Omega} \cdot \boldsymbol{k}) \ll 1$) then C_g is approximately parallel to the rotation axis $\boldsymbol{\Omega}$, so that information concerning slow disturbances is communicated in this direction. This is the mechanism which underlies and mediates the seemingly magical Proudman–Taylor theorem whereby slow fluid motions tend to be invariant parallel to the rotation axis in a rapidly-rotating fluid. Finally, it is worth emphasizing that Inertial waves are dispersive, anisotropic and are characterized by circular particle motions.

3. Alfvén waves and magnetic tension

3.1. The Lorentz force, magnetic field lines and Magneto-Inertial oscillations

Next, let us consider how waves can arise due to the presence of a magnetic field permeating an electrically conducting fluid that is not rotating. A simple thought experiment [22] is useful for illustrating the physical mechanism at work. Imagine a uniform magnetic field is permeating a perfectly conducting fluid, and a uniform flow is initially normal to the magnetic field lines. According to the frozen flux theorem, fluid flow will distort the magnetic field lines so they become curved. The curvature of magnetic field lines produces a magnetic (Lorentz) force on the fluid in a direction opposing further curvature, as specified by Lenz's law. Following Newton's second law, this Lorentz force then changes the momentum of the fluid, pushing it (and consequently the magnetic field lines) back towards the original, undistorted state.

As the curvature of the magnetic field lines increases, so does the strength of the restoring force. Eventually the Lorentz force becomes strong enough to reverse the direction of the fluid flow. Magnetic field lines are pushed back to their original, undistorted configuration and the Lorentz force associated with their curvature weakens until the field lines become straight again. The sequence of flow causing field line distortion and field line distortion exerting a force on the fluid now repeats, but with the initial flow (a consequence of fluid inertia) now present in the opposite direction. In the absence of dissipation this Magneto-Inertial oscillation will continue indefinitely. Figure 1 shows one complete cycle of such an oscillation. If a magnetic field line is disturbed in this manner at one location, then a disturbance will travel along the field line away from this point

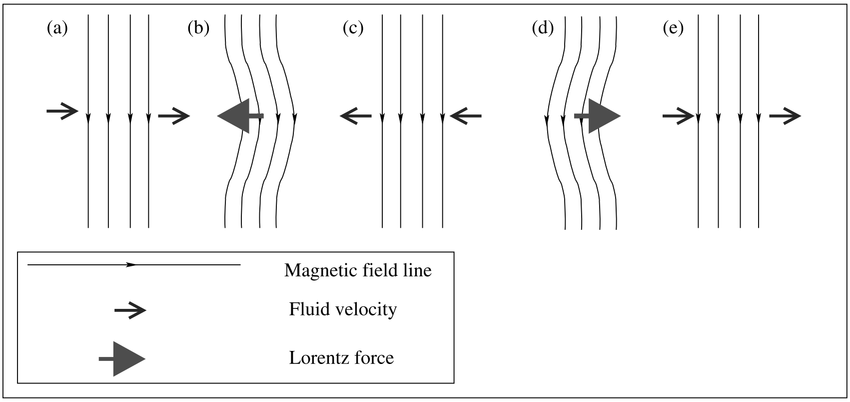

Fig. 1. Schematic illustration of a complete cycle of the basic oscillation mechanism underlying Alfvén waves.

due to the coupling provided between adjacent fluid parcels by the magnetic field line which resists strong curvature. Such travelling disturbances arising from the balance between magnetic (Lorentz) forces and inertial effects are known as Alfvén waves after Hannes Alfvén who discovered them [5].

Additional physical intuition concerning Alfvén waves can be obtained by an analogy between the response of a magnetic field line distorted by fluid flow and the response of an elastic string when plucked. Both rely on tension as a restoring force, elastic tension in the case of the string and magnetic tension in the case of the magnetic field line. Both result in transverse waves propagating in directions perpendicular to their displacement. When visualizing Alfvén waves it can be helpful to think of a fluid as being endowed with a pseudo-elastic nature by the presence of a magnetic field, and consequently supporting transverse waves. Lucid accounts of the basic principles of Alfvén waves can be found in the books by Alfvén and Fälthammar [6] and Davidson [22].

3.2. The Alfvén wave equation

To deduce the properties of Alfvén waves in a more quantitative manner, one follows the classical approach of deriving a wave equation. Consider a uniform, steady, magnetic field $\boldsymbol{B_0}$ imposed in infinite, homogeneous, incompressible, non-rotating electrically conducting fluid of density ρ and magnetic permeability μ. For simplicity, viscosity is neglected and the fluid is assumed to be perfectly conducting.

Now imagine that the fluid is perturbed by an infinitesimally small flow $\boldsymbol{u}$ inducing a perturbation magnetic field $\boldsymbol{b}$. Ignoring terms that are quadratic in small quantities, the linearized equations describing conservation of momentum and the evolution of the magnetic fields (by frozen flux advection) are

$$\underbrace{\frac{\partial \boldsymbol{u}}{\partial t}}_{\substack{\text{Inertial}\\ \text{acceleration}}} = \underbrace{-\frac{1}{\rho}\nabla p}_{\substack{\text{Combined mechanical and}\\ \text{magnetic pressure gradient}}} + \underbrace{\frac{1}{\rho\mu}\left(\boldsymbol{B_0}\cdot\nabla\right)\boldsymbol{b}.}_{\substack{\text{Lorentz acceleration}\\ \text{due to magnetic tension}}} \tag{3.1}$$

$$\underbrace{\frac{\partial \boldsymbol{b}}{\partial t}}_{\substack{\text{Change in the}\\ \text{magnetic field}}} = \underbrace{\left(\boldsymbol{B_0}\cdot\nabla\right)\boldsymbol{u}.}_{\substack{\text{Stretching of magnetic}\\ \text{field by fluid motion}}} \tag{3.2}$$

Taking the curl ($\nabla\times$) of (3.1) gives an equation describing how the fluid vorticity $\xi = \nabla \times \boldsymbol{u}$ evolves

$$\frac{\partial \boldsymbol{\xi}}{\partial t} = \frac{1}{\rho\mu}\left(\boldsymbol{B_0}\cdot\nabla\right)\left(\nabla\times\boldsymbol{b}\right). \tag{3.3}$$

$\nabla\times$ (3.2) gives

$$\nabla\times\frac{\partial \boldsymbol{b}}{\partial t} = \left(\boldsymbol{B_0}\cdot\nabla\right)\boldsymbol{\xi}. \tag{3.4}$$

To find the wave equation, take a further time derivative of (3.3) so that

$$\frac{\partial^2 \boldsymbol{\xi}}{\partial t^2} = \frac{1}{\rho\mu}\left(\mathbf{B_0}\cdot\nabla\right)\left(\nabla\times\frac{\partial \boldsymbol{b}}{\partial t}\right), \tag{3.5}$$

and then eliminate $\boldsymbol{b}$ using an expression for $\frac{1}{\rho\mu}\left(\boldsymbol{B_0}\cdot\nabla\right)\left(\nabla\times\partial\boldsymbol{b}/\partial t\right)$ in terms of $\boldsymbol{\xi}$ obtained by operating with $\frac{1}{\rho\mu}\left(\boldsymbol{B_0}\cdot\nabla\right)$ on (3.4)

$$\frac{1}{\rho\mu}\left(\boldsymbol{B_0}\cdot\nabla\right)\left(\nabla\times\frac{\partial \boldsymbol{b}}{\partial t}\right) = \frac{1}{\rho\mu}\left(\boldsymbol{B_0}\cdot\nabla\right)^2\boldsymbol{\xi}. \tag{3.6}$$

When this is substituted into (3.5) the Alfvén wave equation is obtained

$$\frac{\partial^2 \boldsymbol{\xi}}{\partial t^2} = \frac{1}{\rho\mu}\left(\boldsymbol{B_0}\cdot\nabla\right)^2\boldsymbol{\xi}. \tag{3.7}$$

The term on the right hand side arises from the restoring force caused by the stretching of magnetic field lines.

3.3. Alfvén wave dispersion relation and properties

Substituting a simple plane wave solution of the form $\boldsymbol{\xi} = \mathcal{R}e\{\widehat{\boldsymbol{\xi}}\, e^{i(\mathbf{k}\cdot\mathbf{r}-\omega\mathbf{t})}\}$ into the Alfvén wave equation (3.7), valid solutions are possible provided that

$$\omega^2 = \frac{B_0^2(\boldsymbol{k}\cdot\widehat{\boldsymbol{B_0}})^2}{\rho\mu}, \tag{3.8}$$

where $\widehat{\boldsymbol{B_0}} = \boldsymbol{B_0}/\,|B_0|$.

(3.8) is the dispersion relation for Alfvén waves. It is a quadratic equation in ω, so the well known quadratic formula can be used to find explicit solutions for ω, which are

$$\omega = \pm v_A(\boldsymbol{k}\cdot\widehat{\boldsymbol{B_0}}), \tag{3.9}$$

where v_A known is the Alfvén velocity

$$v_A = \frac{B_0}{(\rho\mu)^{1/2}}. \tag{3.10}$$

This derivation illustrates that the Alfvén velocity is the speed at which an Alfvén wave propagates along magnetic field lines. Alfvén waves are non-dispersive because their phase velocity is independent of $|k|$ and equal to their group velocity are equal. Alfvén waves are however anisotropic, with their properties dependent on the angle between the background magnetic field and the wave propagation direction. Finally, it should be remarked that particle motions associated with simple Alfvén waves are linearly polarized.

4. Magnetic Coriolis (MC) waves

4.1. Force balances in rapidly-rotating, hydromagnetic fluids

Considering a system that is both rapidly-rotating and strongly influenced by a magnetic field, both magnetic field tension and vortex tension must be considered leading to a combination of Alfvén waves and Inertial waves. Lehnert [66] demonstrated that in the simplest case when the rotation axis and the background magnetic field are aligned, two scenarios are possible:

1. **Lorentz and Coriolis forces act together: Fast MC waves**
   Circularly polarized motion of the velocity perturbation, caused by the rotation of the fluid, occurs in an anti-clockwise direction. Therefore the Coriolis force acts in the same direction as the restoring Lorentz force caused by the

deviation of the fluid element (and magnetic field) from its undisturbed position. The restoring force due to the sum of the Lorentz and Coriolis forces is therefore strong and causes rapid motion and significant inertial acceleration. The resulting hydromagnetic waves are typically faster than pure Alfvén waves and are therefore known as fast MC waves.

2. **Lorentz and Coriolis forces in opposition: Slow MC waves**
   On the other hand, if the circularly polarized motion of the velocity perturbation occurs in an clockwise direction, the Coriolis force acts in the opposite direction to the restoring Lorentz force. The restoring force is thus weakened and the resulting particle motions are slow and do not involve significant inertial acceleration. These hydromagnetic waves are typically slower than pure Alfvén waves and are known as slow MC waves. Note that the kinetic energy associated with slow MC waves is much less than that associated with fast MC waves, though the slow waves still involve significant magnetic energy.

In general, the rotation axis and background magnetic field will not be parallel and the situation will be more complex. Nevertheless, the physical picture of circular particle motions involving Lorentz and Coriolis forces combining to produce fast and slow MC modes remains intact.

4.2. The MC wave equation

To derive the MC wave equation for a rapidly-rotating fluid permeated by a strong magnetic field in the absence of viscous and magnetic diffusion, the starting point is the linearized momentum equation including Coriolis, Lorentz and inertial acceleration

$$\frac{\partial \boldsymbol{u}}{\partial t} + 2(\boldsymbol{\Omega} \times \boldsymbol{u}) = -\frac{1}{\rho}\nabla p + \frac{1}{\rho\mu}(\boldsymbol{B_0} \cdot \nabla)\boldsymbol{b}, \tag{4.1}$$

and the frozen flux induction equation

$$\frac{\partial \boldsymbol{b}}{\partial t} = (\boldsymbol{B_0} \cdot \nabla)\boldsymbol{u}. \tag{4.2}$$

Taking the curl of each of these, using the solenoidal properties of the magnetic and velocity fields, and recognizing the vorticity $\boldsymbol{\xi} = \nabla \times \boldsymbol{u}$ leads to

$$\frac{\partial \boldsymbol{\xi}}{\partial t} - 2(\boldsymbol{\Omega} \cdot \nabla)\boldsymbol{u} = \frac{1}{\rho\mu}(\boldsymbol{B_0} \cdot \nabla)(\nabla \times \boldsymbol{b}), \tag{4.3}$$

and

$$\frac{\partial (\nabla \times \boldsymbol{b})}{\partial t} = (\boldsymbol{B_0} \cdot \nabla)\boldsymbol{\xi}. \tag{4.4}$$

A further time derivative of (4.3) and substituting from (4.4) enables these to be combined into a single vorticity equation

$$\frac{\partial^2 \boldsymbol{\xi}}{\partial t^2} - 2(\boldsymbol{\Omega}\cdot\nabla)\frac{\partial \boldsymbol{u}}{\partial t} = \frac{1}{\rho\mu}(\boldsymbol{B_0}\cdot\nabla)^2\boldsymbol{\xi}. \tag{4.5}$$

Taking the curl of this and using the property $\nabla\times\boldsymbol{\xi} = \nabla\times(\nabla\times\boldsymbol{u}) = -\nabla^2\boldsymbol{u}$ gives

$$-2(\boldsymbol{\Omega}\cdot\nabla)\frac{\partial \boldsymbol{\xi}}{\partial t} = \left(\frac{\partial^2}{\partial t^2} - \frac{1}{\rho\mu}(\boldsymbol{B_0}\cdot\nabla)^2\right)\nabla^2\boldsymbol{u}. \tag{4.6}$$

Finally taking $\partial/\partial t$ (4.5) gives an expression for $\partial\boldsymbol{\xi}/\partial t$ that can be substituted into (4.6) to eliminate $\boldsymbol{\xi}$ leaving a single equation for the perturbation velocity $\boldsymbol{u}$. This is known as the Magnetic Coriolis (MC) or Alfvén-Inertial wave equation [3, 22, 66],

$$\left(\frac{\partial^2}{\partial t^2} - \frac{1}{\rho\mu}(\boldsymbol{B_0}\cdot\nabla)^2\right)^2\nabla^2\boldsymbol{u} = -4(\boldsymbol{\Omega}\cdot\nabla)^2\frac{\partial^2\boldsymbol{u}}{\partial t^2}. \tag{4.7}$$

4.3. MC wave dispersion relation and properties

The MC wave equation is considerably more complex than the Alfvén and Inertial wave equations: it is 4th order in the time derivative, leading us to expect the existence of 4 different modes. These modes can be identified as before by substituting a plane wave anstatz $\boldsymbol{u} = \mathcal{R}e\{\widehat{\boldsymbol{u}}e^{i(\boldsymbol{k}\cdot\boldsymbol{r}-\omega t)}\}$ into the wave equation (4.7) which yields

$$\left(\frac{(\boldsymbol{B_0}\cdot\boldsymbol{k})^2}{\rho\mu} - \omega^2\right)^2 k^2 - 4(\boldsymbol{\Omega}\cdot\boldsymbol{k})^2\omega^2 = 0. \tag{4.8}$$

Taking the final term to the right hand side, dividing through by k^2 and taking the square root it can be seen that the possible solutions are

$$\frac{(\boldsymbol{B_0}\cdot\boldsymbol{k})^2}{\rho\mu} - \omega^2 = \pm\frac{2(\boldsymbol{\Omega}\cdot\boldsymbol{k})}{|k|}\omega. \tag{4.9}$$

These are two quadratic equations in ω: each can be solved using the usual quadratic formula to obtain the four solutions

$$\omega_{MC} = \pm\frac{(\boldsymbol{\Omega}\cdot\boldsymbol{k})}{k} \pm \left(\frac{(\boldsymbol{\Omega}\cdot\boldsymbol{k})^2}{k^2} + \frac{(\boldsymbol{B_0}\cdot\boldsymbol{k})^2}{\rho\mu}\right)^{1/2}. \tag{4.10}$$

When the two signs are the same polarity, then 2 fast MC waves (with Lorentz and Coriolis forces reinforcing each other) travelling in opposite directions are obtained. When the two signs are of different polarity, 2 slow MC waves (with Lorentz and Coriolis forces opposing each other) travelling in opposite directions are obtained.

Note that in the limit where rotation becomes unimportant ($\mathbf{\Omega} \to 0$) the Alfvén wave dispersion relation $\omega = \pm(\boldsymbol{B_0} \cdot \boldsymbol{k})/\sqrt{\rho\mu}$ is recovered, while in the opposite limit when magnetic fields are unimportant ($\boldsymbol{B_0} \to 0$) the Inertial wave dispersion relation $\omega = \pm 2(\mathbf{\Omega} \cdot \boldsymbol{k})/k$ is obtained.

If the frequency of Inertial waves is much larger than the frequency of Alfvén waves so that

$$|2(\mathbf{\Omega} \cdot \boldsymbol{k})/k| \gg |(\boldsymbol{B_0} \cdot \boldsymbol{k})/\sqrt{\rho\mu}| \tag{4.11}$$

(i.e. if rotation is sufficiently rapid) then it is possible to carry out a Taylor series expansion of (4.10) in the small quantity $k^2(\boldsymbol{B_0} \cdot \boldsymbol{k})^2/4(\mathbf{\Omega} \cdot \boldsymbol{k})^2\rho\mu$. One then finds a very clear splitting of the fast and slow wave frequencies such that the leading order expressions for the dispersion relations are

$$\omega_{MC}^{f} = \pm\frac{(2\mathbf{\Omega} \cdot \boldsymbol{k})}{k}\left(1 + \frac{k^2(\boldsymbol{B_0} \cdot \boldsymbol{k})^2}{4(\mathbf{\Omega} \cdot \boldsymbol{k})^2\rho\mu}\right), \tag{4.12}$$

and

$$\omega_{MC}^{s} = \pm\frac{k(\boldsymbol{B_0} \cdot \boldsymbol{k})^2}{2(\mathbf{\Omega} \cdot \boldsymbol{k})\rho\mu}. \tag{4.13}$$

Remembering that $k^2(\boldsymbol{B_0} \cdot \boldsymbol{k})^2/4(\mathbf{\Omega} \cdot \boldsymbol{k})^2\rho\mu$ is a small quantity, it is observed in this limit that the fast MC wave (ω_{MC}^{f}) is essentially an Inertial wave slightly modified by the presence of a magnetic field such that the wave frequency is higher than that of a pure inertial wave. Thus frequencies greater than 2Ω that are impossible for pure inertial waves are possible for fast MC waves. This fact can be a useful diagnostic property when trying to determine the type of waves present in an experiment or simulation.

The slow MC wave (ω_{MC}^{s}) that emerges in this limit emerges signifies a new fundamental timescale for rapidly-rotating, hydromagnetic systems

$$\tau_{MC} = \frac{2\Omega\rho\mu L^2}{B_0^2}, \tag{4.14}$$

where L is the lengthscale associated with a slow MC wave disturbance. Note that this is the square of the Alfvén wave timescale divided by the inertial wave timescale. Thus, the faster the rotation, the longer τ_{MC} becomes, while the stronger the magnetic field is, the shorter τ_{MC} becomes. Physically, this is because the Lorentz force is the fundamental restoring mechanism, with the Coriolis force acting to oppose it. It is worth reiterating that inertia plays no role in the slow MC waves in this limit: they are a consequence of a slowly evolving push and pull between the Lorentz force and the Coriolis force. Slow MC waves are therefore sometimes also called magnetostrophic waves [74].

Slow MC waves are both anisotropic and dispersive with their phase and group velocity taking the form

$$C_{\mathrm{ph}} = \frac{(\boldsymbol{B_0} \cdot \boldsymbol{k})^2}{2(\boldsymbol{\Omega} \cdot \boldsymbol{k})k\rho\mu}\boldsymbol{k}, \tag{4.15}$$

$$C_{\mathrm{g}} = \frac{k(\boldsymbol{B_0} \cdot \boldsymbol{k})^2}{2(\boldsymbol{\Omega} \cdot \boldsymbol{k})\rho\mu}\left(\frac{\boldsymbol{k}}{k} + \frac{2\boldsymbol{B_0}}{(\boldsymbol{k} \cdot \boldsymbol{B_0})} - \frac{\boldsymbol{\Omega}}{(\boldsymbol{k} \cdot \boldsymbol{\Omega})}\right). \tag{4.16}$$

The slow MC wave has attracted the attention of geophysicists because $\tau_{MC} \sim 300$ years for plausible geophysical parameters of $2\pi/k \sim 2.75 \times 10^6$ m and $B_0 \sim 5 \times 10^{-3}$ T). This is coincident with timescale of observed wave-like geomagnetic secular variation signals [42].

Hide (see Appendix A) and Malkus (see Appendix B) have extended models of MC waves to take account of spherical geometry. Hide used a β-plane approach similar to that commonly employed in meteorology and oceanography. Malkus used a special cylindrically symmetric, force free, imposed magnetic field in full sphere geometry to simply the spherical MC wave problem to a complex variable generalization of the well known Inertial wave problem in a sphere.

5. Magnetic Archimedes Coriolis (MAC) waves

5.1. Influence of density stratification and convective instability

In this section, the generalization of MC waves to the case including density stratification that can drive convection is described. Density variations are introduced by imposing a background temperature gradient, this can produce both stable stratification or convective instability. The Boussinesq approximation [21] to the heat and momentum equations is also employed for simplicity. The wave motions resulting in this scenario, when magnetic fields, density gradient and rapid rotation are present, are known as Magnetic Archimedes Coriolis (MAC) waves.

The dimensional linearized equations describing Boussinesq rotating magnetoconvection in an infinite plane layer geometry are

$$2\boldsymbol{\Omega} \times \boldsymbol{u} = -\frac{1}{\rho_0}\nabla p + \frac{1}{\mu\rho_0}\left(\mathbf{B_0} \cdot \nabla\right) \boldsymbol{b} + \gamma\alpha\Theta\widehat{\boldsymbol{z}}, \tag{5.1}$$

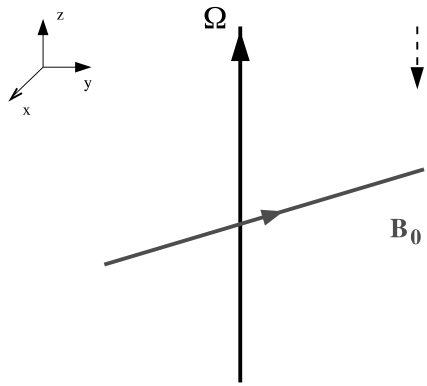

Fig. 2. Infinite plane layer setup for MAC waves. Gravity is imposed parallel to the rotation axis (as is the imposed temperature gradient, not shown). The imposed magnetic field is uniform but at an arbitrary angle to the rotation axis.

$$\frac{\partial \boldsymbol{b}}{\partial t} = (\mathbf{B_0} \cdot \nabla)\, \boldsymbol{u}, \tag{5.2}$$

$$\frac{\partial \Theta}{\partial t} = -\beta'(\widehat{\boldsymbol{z}} \cdot \boldsymbol{u}). \tag{5.3}$$

Cartesian co-ordinates $(\widehat{\boldsymbol{x}}, \widehat{\boldsymbol{y}}, \widehat{\boldsymbol{z}})$ have been employed with the axis of rotation chosen to lie along $\widehat{\boldsymbol{z}}$ (see Fig. 2). The imposed magnetic field is chosen to be uniform (i.e. $\nabla \boldsymbol{B_0} = 0$) but in an arbitrary direction, so $\boldsymbol{B_0} = (B_{0x}\widehat{\boldsymbol{x}} + B_{0y}\widehat{\boldsymbol{y}} + B_{0z}\widehat{\boldsymbol{z}})$. The uniform background temperature gradient is $\nabla T_0 = \beta'\widehat{\boldsymbol{z}}$. In a gravity field $\boldsymbol{g} = -\gamma\widehat{\boldsymbol{z}}$, the buoyancy force is therefore $\rho_0\gamma\alpha\Theta$ in the $\widehat{\boldsymbol{z}}$ direction, where $T = T_0 + \Theta$ and α is the thermal expansivity. Note that $\beta' \gg 0$ implies less dense fluid overlies more dense fluid (stable stratification) while $\beta' \ll 0$ implies colder and more dense fluid overlies hotter and less dense fluid, a situation that is unstable to convection.

Note that in (5.1) to (5.3) the inertial term $(\partial \boldsymbol{u}/\partial t)$ as well as viscous, magnetic and thermal diffusion have been ignored, in order to focus attention on the essential physics involving the Lorentz (Magnetic), buoyancy (Archimedes) and Coriolis forces. Ignoring the inertial term in the previous section would have resulted in only the slow MC mode being obtained, a similar filtering out of the fast mode occurs here. ρ_0 rather than ρ is now used to represent the fluid density to emphasize that the Boussinesq approximation has been made.

Taking $\frac{\partial}{\partial t}\nabla\times$ (5.1) to eliminate pressure gives

$$2(\boldsymbol{\Omega}\cdot\nabla)\frac{\partial \boldsymbol{u}}{\partial t} = \frac{(\mathbf{B_0}\cdot\nabla)}{\mu\rho_0}\frac{\partial}{\partial t}(\nabla\times\boldsymbol{b}) + \gamma\alpha\frac{\partial}{\partial t}(\nabla\times\Theta\widehat{\boldsymbol{z}}), \tag{5.4}$$

while taking $\nabla\times$ (5.2) yields

$$\frac{\partial}{\partial t}(\nabla\times\boldsymbol{b}) = (\mathbf{B_0}\cdot\nabla)\,(\nabla\times\boldsymbol{u}). \tag{5.5}$$

Substituting from (5.5) into (5.4) for $\frac{\partial}{\partial t}(\nabla\times\boldsymbol{b})$ gives a vorticity equation quantifying the MAC balance with terms arising from Coriolis force on the left hand side and terms arising from the magnetic and buoyancy forces on the right hand side

$$2(\boldsymbol{\Omega}\cdot\nabla)\frac{\partial \boldsymbol{u}}{\partial t} = \frac{(\mathbf{B_0}\cdot\nabla)^2}{\mu\rho_0}(\nabla\times\boldsymbol{u}) + \gamma\alpha\frac{\partial}{\partial t}(\nabla\times\Theta\widehat{\boldsymbol{z}}). \tag{5.6}$$

Operating on this with $\frac{(\mathbf{B_0}\cdot\nabla)^2}{\mu\rho_0}\nabla\times$ gives

$$\begin{aligned}2(\boldsymbol{\Omega}\cdot\nabla)\frac{\partial}{\partial t}\frac{(\mathbf{B_0}\cdot\nabla)^2}{\mu\rho_0}(\nabla\times\boldsymbol{u}) &= \left[\frac{(\mathbf{B_0}\cdot\nabla)^2}{\mu\rho_0}\right]^2(\nabla\times(\nabla\times\boldsymbol{u}))\\ &\quad+\gamma\alpha\frac{(\mathbf{B_0}\cdot\nabla)^2}{\mu\rho_0}\frac{\partial}{\partial t}(\nabla\times(\nabla\times\Theta\widehat{\boldsymbol{z}})).\end{aligned} \tag{5.7}$$

(5.7) can be simplified by noting that $\frac{(\mathbf{B_0}\cdot\nabla)^2}{\mu\rho_0}(\nabla\times\boldsymbol{u})$ can be eliminated by using (5.6) again, and remembering that for an incompressible fluid $\nabla\times(\nabla\times\boldsymbol{u}) = -\nabla^2\boldsymbol{u}$. Then taking the dot product of (5.7) with $\widehat{\boldsymbol{z}}$ one also recognizes that $\widehat{\boldsymbol{z}}\cdot(\nabla\times\Theta\widehat{\boldsymbol{z}}) = 0$ and $\widehat{\boldsymbol{z}}\cdot(\nabla\times(\nabla\times\Theta\widehat{\boldsymbol{z}})) = -(\frac{\partial^2}{\partial x^2}+\frac{\partial^2}{\partial y^2})\Theta = -\nabla_H^2\Theta$. Carrying out these operations it is found that

$$4(\boldsymbol{\Omega}\cdot\nabla)^2\frac{\partial^2}{\partial t^2}u_z = -\left[\frac{(\mathbf{B_0}\cdot\nabla)^2}{\mu\rho_0}\right]^2\nabla^2 u_z - \gamma\alpha\frac{(\mathbf{B_0}\cdot\nabla)^2}{\mu\rho_0}\nabla_H^2\frac{\partial\Theta}{\partial t}. \tag{5.8}$$

Finally, making use of the linearized heat equation (5.3) to eliminate $\frac{\partial\Theta}{\partial t}$, a sixth order equation in u_z is obtained. This is the diffusionless MAC wave equation [9]

$$\left(4(\boldsymbol{\Omega}\cdot\nabla)^2\frac{\partial^2}{\partial t^2} + \left[\frac{(\mathbf{B_0}\cdot\nabla)^2}{\mu\rho_0}\right]^2\nabla^2 - \gamma\alpha\beta'\frac{(\mathbf{B_0}\cdot\nabla)^2}{\mu\rho_0}\nabla_H^2\right)u_z = 0. \tag{5.9}$$

Properties of diffusionless MAC waves can now be deduced by substitution of plane wave solutions of the form $u_z = \mathcal{R}e\{\widehat{u_z} e^{i(\mathbf{k}\cdot\mathbf{r}-\omega\mathbf{t})}\}$, where $\mathbf{k}$ is the wavevector and ω is the angular frequency

$$4(\boldsymbol{\Omega}\cdot\boldsymbol{k})^2\omega^2 - \left[\frac{(\mathbf{B_0}\cdot\boldsymbol{k})^2}{\mu\rho_0}\right]^2 k^2 - \frac{(\mathbf{B_0}\cdot\boldsymbol{k})^2}{\mu\rho_0}\gamma\alpha\beta'(k_x^2+k_y^2) = 0. \tag{5.10}$$

This expression can be written more concisely by observing that terms in it correspond to characteristic angular frequencies for Alfvén waves (see Section 3), internal gravity waves in a thermally stratified fluid, and Inertial waves (see Section 2), respectively defined as

$$\omega_M^2 = \frac{(\mathbf{B_0}\cdot\boldsymbol{k})^2}{\mu\rho_0}, \qquad \omega_A^2 = \frac{\gamma\alpha\beta'(k_x^2+k_y^2)}{k^2}, \qquad \omega_C^2 = \frac{4(\boldsymbol{\Omega}\cdot\boldsymbol{k})^2}{k^2}. \tag{5.11}$$

Using these simplifies (5.10) to

$$\omega_C^2\omega^2 - \omega_M^4 - \omega_M^2\omega_A^2 = 0. \tag{5.12}$$

Solving for ω gives the MAC wave dispersion relation which must be satisfied by the angular frequency and wavevectors of plane MAC waves [9, 93]

$$\omega_{\mathrm{MAC}} = \pm\frac{\omega_M^2}{\omega_C}\left(1+\frac{\omega_A^2}{\omega_M^2}\right)^{1/2} = \pm\omega_{MC}^s\left(1+\frac{\omega_A^2}{\omega_M^2}\right)^{1/2}. \tag{5.13}$$

Due to the importance of this result, for completeness it is also worth stating the full expression which is

$$\omega_{\mathrm{MAC}} = \pm\frac{k\,(\mathbf{B_0}\cdot\boldsymbol{k})^2}{2\rho_0\mu(\boldsymbol{\Omega}\cdot\boldsymbol{k})}\left(1+\frac{\gamma\alpha\beta'\rho_0\mu(k_x^2+k_y^2)}{k^2\,(\mathbf{B_0}\cdot\boldsymbol{k})^2}\right)^{1/2}. \tag{5.14}$$

An alternative derivation of this relation is given by Soward and Dormy [94] who follow Braginsky [10] in using an elegant formulation in terms of the displacement vector of the wave perturbations. This approach is useful for clearly showing how MAC waves are associated with elliptical particle motions. The more pedestrian derivation given above is preferred here because it involves quantities that are more straight-forward to interpret physically, and because links to simpler forms of waves are more transparent.

Note that (5.14) is singular if $\mathbf{B_0}\cdot\boldsymbol{k} = \mathbf{0}$ or if $\boldsymbol{\Omega}\cdot\boldsymbol{k} = 0$, so diffusionless MAC waves cannot propagate normal to magnetic field lines or to the rotation axis. The frequency of MAC waves depends strongly on their wavelength (i.e., they are highly dispersive) and on their direction compared to the direction of the rotation axis and the magnetic field direction (i.e., they are anisotropic). When buoyancy forces are absent ($\alpha = 0$), the dispersion relation simplifies to that for slow MC waves (remember the inertial terms were filtered out in this derivation).

The important extra ingredient introduced in the presence of thermal stratification is that if the background temperature gradient $\beta' \ll 0$ then ω_A^2 will be negative so ω_{MAC} will have an imaginary part, thus there will a growing or unstable mode. This is of course a thermally-driven (convective) instability: MAC waves in this case are the form in which rotating magnetoconvection is manifested. On the other hand, if the thermal stratification is stable with $\beta' \gg 0$ then this imaginary part is absent and the MAC waves are stable free waves. In the latter case the stable stratification acts increase the frequency of the MAC waves compared to MC waves. A complete and rigorous analysis of the growth rates of MAC waves requires one to assume that ω is complex and to look at the real and imaginary parts of the resulting dispersion relation.

5.2. *Influence of diffusion*

Thus far, the influence of any form of dissipation (viscous, magnetic or thermal diffusion) has been neglected in order to simplify both the mathematical analysis and the physical picture. In this section these effects are re-introduced. Naively, the presence of dissipation might be expected to merely damp disturbances and irreversibly transform energy to an unusable form. Although such processes certainly occur, the presence of diffusion also has more unexpected consequences.

Perhaps most importantly, diffusion adds extra degrees of freedom to the system, permitting exchange of heat, momentum and magnetic fields with the surroundings. This can aid the destabilization of waves that were stable in the absence of diffusion (see [84, 85] and [2]). Mathematically, the diffusion coefficients appear as part of the complex dispersion relation determining the growth rate, and not just in a simple dissipative manner. The result is that MAC/MC wave instability can occur for smaller unstable density gradients (or even for stable density gradients) compared to when no diffusion is present. Since diffusion is crucial for determining the fastest growing modes, it must be included if one wishes to determine which MAC wave modes will dominate the solution for a specified temperature gradient.

The diffusive instability mechanism works most effectively when the oscillation frequency matches the rate of the dominant diffusion process. The timescale of the most unstable waves is therefore often similar to that of the diffusion process which is facilitating the instability [2]. Diffusion thus introduces new preferred timescales for unstable MAC waves: those of thermal or magnetic diffusion, in addition to the diffusionless MC/MAC wave timescale.

To include diffusion in the mathematical description of MAC waves, it is necessary to replace the operator $\frac{\partial}{\partial t}$ by $\left(\frac{\partial}{\partial t} - \nu\nabla^2\right)$ in the momentum equation, $\left(\frac{\partial}{\partial t} - \eta\nabla^2\right)$ in the induction equation, and $\left(\frac{\partial}{\partial t} - \kappa\nabla^2\right)$ in the heat equation. Retaining the acceleration (inertial) term in the momentum equation and including the Laplacian diffusion terms before the substitution of plane wave solutions results in a rather more complicated, explicitly complex, dispersion relation for diffusive MAC waves in a plane layer [74, 93, 94],

$$\begin{aligned}\left(\omega_C^2(\omega + i\eta k^2)^2 - \left[(\omega + i\nu k^2)(\omega + i\eta k^2) - \omega_M^2\right]^2\right)(\omega + i\kappa k^2)\\ + \omega_A^2(\omega + i\eta k^2)\left[(\omega + i\nu k^2)(\omega + i\eta k^2) - \omega_M^2\right] = 0.\end{aligned} \tag{5.15}$$

More detail on diffusive MC waves with and without the inclusion of inertia, and their troublesome impact on geodynamo simulations can be found in [99] and [54].

6. MAC waves in spherical geometry

6.1. Quasi-geostrophic (QG) models of MAC waves

The simple models presented in previous sections have ignored the presence of any boundaries, in an attempt to focus on the essential physics. However, many geophysical and astrophysical systems involve spherical confining geometry. In this section, an analytic 'quasi-geostrophic' (QG) MAC wave model capturing the important latitudinal variations in planetary vorticity (the origin of Rossby waves) is outlined, before MAC wave solutions in full spherical geometry derived by numerical computations are presented in the next section.

Quasi-geostrophic (QG) models of MAC waves (also known in the literature as QG models of rotating magnetoconvection) were first developed by Busse [14] and Soward [93] building Hide's pioneering study of MC Rossby waves [52] (also see Appendix A). The setup of the QG model is shown in Fig. 3. The mathematical details of the model are set out in Appendix C.

The crucial new physics in the QG model compared to plane layer models arises from its sloping upper and lower boundaries. This geometry mimics the changes experienced by a columnar disturbance[3] as it moves latitudinally in a spherical shell geometry [13, 15, 52]. The sloping boundaries cause stretching or compression of a columnar disturbance as it moves in the direction perpendicular to the rotation axis. But compressed columns acquire anticyclonic vorticity, while stretched columns acquire cyclonic vorticity due to conservation of potential vorticity [77]. The acquired or lost vorticity causes displaced columns to

[3]The natural structure for slow motions in a rapidly-rotating fluid by virtue of the Proudman–Taylor theorem [49].

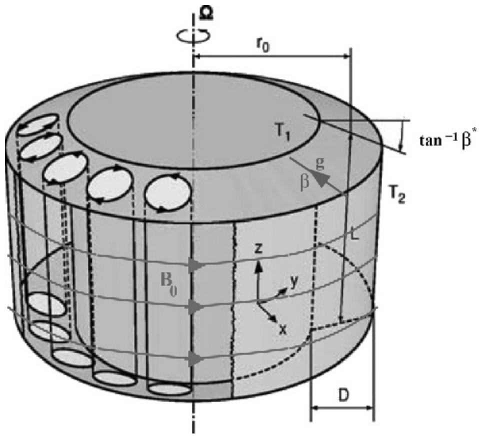

Fig. 3. Setup of Quasi-Geostrophic sloping annulus model for studying 2D MAC waves that are structurally invariant parallel to the rotation axis. It includes radial gravity, a radial temperature gradient and an azimuthal imposed magnetic field. Analysis is carried out in a local co-ordinate system with $\hat{\boldsymbol{z}}$ in the direction of the rotation axis, $\hat{\boldsymbol{y}}$ in the prograde azimuthal direction and $\hat{\boldsymbol{x}}$ in the cylindrically radial direction. This figure is modified from Busse (2002) [15].

drift back towards their initial position, while also drifting azimuthally. This is the basis of the Rossby wave propagation mechanism (e.g. see Busse [15], his Fig. 2) and is the reason Hide's model (see Appendix A) also supports Rossby waves. The QG model therefore includes the Rossby wave mechanism important for slow motions in a spherical geometry via its sloping boundaries: this important physical effect is ignored in plane layer models.

Formally, in the QG approximation, the momentum, induction and heat equations are integrated in the direction parallel to the rotation axis, along which only small variations are expected due to the rapid rotation of the system. This results in equations for the evolution of z-averaged axial vorticity perturbation, electric current density perturbation and temperature perturbation (see Appendix C for details) in a 2D plane. The effect of sloping boundaries and the associated deviations from geostrophy are taken into account by respecting conservation of mass at the boundaries. Manipulating the resulting equations to produce a single wave equation, and substituting a simple wave anstatz $\sim e^{i(kx+ky-\omega t)}$, assuming the wavenumber in the $\hat{\boldsymbol{x}}$ and $\hat{\boldsymbol{y}}$ direction to be the same, leads to the following complex dispersion relation,

$$E(-i\omega + k^2) + \frac{i\beta^*}{k} = \frac{E\,Ra}{-i\,Pr\,\omega + k^2} - \frac{\Lambda k^2}{-i\,Pr_m\omega + k^2}, \qquad (6.1)$$

where non-dimensionalization by the depth of the annulus L and the viscous diffusion timescale has been carried out and the resulting control parameters are

$$\Lambda = \frac{B_0^2}{2\Omega\mu\rho_0\eta} = \frac{\text{Magnetic diffusion timescale}}{\text{slow MC timescale}}, \tag{6.2}$$

$$Pr = \frac{\nu}{\kappa} = \frac{\text{Thermal diffusion timescale}}{\text{Viscous diffusion timescale}}, \tag{6.3}$$

$$Pr_m = \frac{\nu}{\eta} = \frac{\text{Magnetic diffusion timescale}}{\text{Viscous diffusion timescale}}, \tag{6.4}$$

$$E = \frac{\nu}{2\Omega L^2} = \frac{\text{Rotation timescale}}{\text{Viscous diffusion timescale}}, \tag{6.5}$$

$$Ra = \frac{\gamma\,\alpha\,|\nabla T_0|\,L^4}{\kappa\nu} = \frac{\text{Buoyant rise timescale in viscous fluid}}{\text{Thermal diffusion timescale}}, \tag{6.6}$$

and β^* is the tangent of the boundary slope. For a full derivation, interested readers should consult Appendix C.

The first term in dispersion relation (6.1) comes from the inertial and viscous effects, the second term results from the Coriolis force (actually it is the β-effect due to the sloping boundary altering the vorticity of columnar disturbances described above). The third term represents thermal (convective) forcing due to the action of gravity on density gradients, and the fourth term describes the influence of the uniform azimuthal magnetic field.

By looking at (6.1) in different limits, different types of waves can be isolated; these give insight into the forms of dynamics contained within the QG model.

1. **Rossby waves.**
   Ignoring thermal driving and the influence of magnetic fields leaving inertia, viscosity and the β-effect arising from column stretching in balance,

$$E(-i\omega + k^2) = -\frac{i\beta^*}{k} \quad => \quad \omega = \frac{\beta^*}{Ek} - i\frac{k^2}{E}. \tag{6.7}$$

   This is the viscous timescale non-dimensionalization version of the dispersion relation expected for free Rossby waves, damped by viscous diffusion effects. These waves travel in the prograde (eastward) direction in the sloping annulus geometry mimicking the scenario outside the tangent cylinder in a thick spherical shell.

2. **Hide's slow MC-Rossby waves.**
Ignoring viscosity, inertia, thermal driving and magnetic diffusion, the β-effect is balanced by the magnetic field which is evolving only through frozen-flux effects,

$$\frac{i\beta^*}{k} = \frac{\Lambda k^2}{-i Pr_m \omega} \quad => \quad \omega = -\frac{\Lambda k^3}{\beta^* Pr_m}. \tag{6.8}$$

This is the dispersion relation expected for Hide's slow MC-Rossby waves, travelling in the retrograde (westward) direction with frequency inversely proportional to the β-effect and proportional to the square of the magnetic field strength (i.e. to Λ).

3. **Magnetically-modified thermal Rossby waves.**
Including the magnetic field but neglecting its time changes, (assuming $\omega Pr_m \ll 1$) while retaining buoyancy force (thermal driving), the dispersion relation reduces to

$$E(-i\omega + k^2) + \frac{i\beta^*}{k} = \frac{E Ra}{-i Pr\, \omega + k^2} - \Lambda. \tag{6.9}$$

Eliminating Ra from the imaginary part of this equation and using the expression for Ra obtained from the real part leads to the relation

$$\omega = \frac{\frac{\beta^* k}{E Pr}}{(1 + Pr^{-1})k^2 + \frac{\Lambda}{E}}. \tag{6.10}$$

When the magnetic field is absent ($\Lambda = 0$), this is the dispersion relation for Busse's thermal Rossby waves [13]. For a weak magnetic field, when $\Lambda \ll 1$, the character of the waves remains essential that of a thermal Rossby wave, but slightly slowed by the influence of the magnetic field.

4. **Thermal magneto-Rossby waves.**
For larger Λ the dispersion relation (6.10) is dominated by Λ / E and it reduces to the form

$$\omega = \frac{\beta^* k}{\Lambda Pr}. \tag{6.11}$$

This type of wave relies crucially on the magnetic field for its existence: it is not just a small correction to thermal Rossby waves, but a new type of motion where the magnetic forces take part in the leading order force balance and viscous forces are less important compared to the case for thermal Rossby waves [14, 34, 93]. It is commonly referred to as a thermal magneto-Rossby wave because it involves a balance between magnetic field effects, the Rossby wave restoring mechanism due to the sloping boundary (β-effect) and is thermally driven. As the magnetic field strength increases these waves have low frequency (in contrast to Hide's slow MC waves, indicating a different role of the magnetic field in the restoring mechanism), while the waves with short wavelengths (larger k) have higher frequency.

5. **Thermal MC-Rossby waves.**
If viscous and inertial terms are again ignored, but if $\omega Pr_m \gg 1$, for example when magnetic diffusion is negligible, then (6.9) reduces to

$$\omega = \frac{\Lambda k^3 \left(Pr - Pr_m\right)}{\beta^* Pr_m^2}. \tag{6.12}$$

This type of wave is essentially Hide's slow MC Rossby wave (hence involves the frozen flux approximation) but thermally driven, so it operates on a much slower timescale than free MC Rossby waves. It is known as the thermal MC Rossby wave. Unfortunately, these waves an unlikely to be relevant for liquid metals because their magnetic diffusion time is much shorter than the thermal diffusion timescale on which these waves operate, so the frozen-flux approximation necessary to obtain them will not be valid. Note however that MC Rossby waves could still occur in liquid metals if they are forced by mechanisms (other than thermal instability) with characteristic timescales that are short compared to that of magnetic diffusion.

To summarize, the QG model includes the essential ingredients for modelling slow motions of a rapidly-rotating fluid in a spherical geometry: motions are then essentially 2D (invariant parallel to the rotation axis) and they undergo changes in vorticity as they move towards and away from the rotation axis (the β-effect). It supports a remarkably rich variety of dynamics; three distinct forms of thermally-driven 2D MAC waves are possible: magnetically-modified thermal Rossby waves, thermal magneto-Rossby waves, and thermal MC Rossby waves. Free Rossby and MC Rossby waves are also possible in the absence of density stratification. When the magnetic field is strong and Pr_m is small, as is the case for liquid metals in planetary cores, thermal magneto-Rossby waves are the most likely form of QG wave to be excited by convection.

The limitations of the QG model should however also be remembered. In particular, it will break down if motions are no longer predominantly 2D (invariant parallel to the rotation axis), for example, (i) where very strong magnetic fields are present; (ii) where the boundary slope approaches infinity in the equatorial regions of a thick spherical shell (i.e. $\beta^* \gg 1$); (iii) when fluid motions are so rapid that inertia becomes dominant and fast, fully 3D, inertial waves rather than slower 2D Rossby waves occur; (iv) when the background magnetic field is no longer uniform, then additional terms are necessary to represent the Lorentz force and magnetically-driven 3D instabilities also become possible. The full spherical model sketched in the next section performs better under all of these circumstances, but must be solved numerically and lacks the understanding power provided by concise analytic solutions provided by the QG framework.

6.2. MAC waves in full sphere geometry

In order to obtain detailed predictions that can be directly related to observations of spherical systems such as Earth's core, it is perhaps best to move to full spherical geometry, due to the limitations of the QG model noted at the end of the previous section.

The problem now becomes a question of efficiently computing the required solutions. This chapter, being focused on physical understanding, is not a suitable place to expound the full numerical details. Only a sketch, giving a flavour of how the spatial structure, frequency and growth rates of wave modes may be obtained is given. Those readers desiring further details should consult chapter 7 of Finlay (2005) [43].

The example calculation presented here involves an imposed magnetic field of the form proposed by Malkus [70] (see Appendix B) with $\boldsymbol{B_0} = B_0 r \sin\theta \widehat{\boldsymbol{\phi}}$. This is a force-free field for which the Lorentz force takes a particularly simple form, which does not drive magnetic instabilities, and is suitable for studying thermally-driven waves. The momentum, induction and heat equations are solved in a full sphere geometry subject to electrically insulating, stress-free and isothermal boundary conditions using a version of the spherical magnetoconvection code of Worland and Jones [57,101] modified by Finlay [43]. The governing equations are non-dimensionalized using the lengthscale $L = r_0$ (radius of the sphere) and the viscous diffusion timescale. The control parameters are therefore again E, Λ, Ra, Pr and Pr_m as defined in (6.2) to (6.6). The equations are linearized around the background magnetic field and a zero velocity field. Working in spherical polar co-ordinates the $\widehat{z}$ component of the curl and double curl of the momentum and induction equations are then taken.

Considering trial wave solutions of a particular azimuthal wavenumber and frequency, the poloidal and toroidal scalars representing the velocity and the magnetic fields and the temperature field are expanded in terms of spherical harmonics horizontally and Chebyshev polynomials radially. The collocation method is then used to formulate the equations on a radial grid. The resulting linear equations can be written in matrix form as a generalized complex eigenvalue problem

$$\lambda \boldsymbol{\mathcal{B}} \boldsymbol{x} = \boldsymbol{\mathcal{A}} \boldsymbol{x}, \tag{6.13}$$

where λ is the complex eigenvalue representing the frequency and growth rate of a particular mode, $\boldsymbol{\mathcal{B}}$ is a matrix of the factors pre-multiplying the $\frac{\partial}{\partial t}$ terms in the system of equations and $\boldsymbol{\mathcal{A}}$ is a matrix containing the pre-factors of all the other terms in the governing equations. $\boldsymbol{x}$ is a vector containing the unknown coefficients. The eigenvalue problem for complex λ (for a choice of m and the control parameters) can be solved, for example using ARPACK routines [43]. One then iterates varying Ra to locate Ra_c for the onset of thermally-driven instability (i.e. the marginally critical mode for which the growth rate is zero), then iterates over m to find that m_c with lowest Ra_c: this then constitutes the most unstable mode for a given set of control parameters. Once a mode of interest is found, its eigenvector defines the spatial structure of the wave while its eigenvalue determines the wave frequency and growth rate.

Here, in contrast to previous sections where the focus was on dispersion relations, the aim is to discuss the spatial structure thermally-driven MAC waves in a sphere. Figures 4, 5 and 6 show examples of the structure of examples of such waves, a magnetically-modified thermal Rossby wave and a thermal magneto-Rossby wave respectively. I have chosen these waves because they were discussed previously in the context of the QG model (hence they are predominantly 2D), but other fully 3D thermal MAC wave modes are also possible at larger Λ in this spherical system.

All these waves involve spatially periodic disturbances of positive and negative anomalies in the velocity, magnetic and temperature fields, though their detailed structure is different. It is worth remarking that the thermal magneto-Rossby modes that are most likely to be driven by convection in planetary core involve large amplitude perturbations of the radial magnetic field close to the outer boundary at low latitudes.

7. Limitations of linear models and towards nonlinear models

All the models discussed so far are linear in the perturbation velocity, magnetic and temperature fields. As such they are fundamentally limited since they ignore: (i) saturation mechanisms, (ii) wave-wave interactions, (iii) wave-mean flow interactions. Nonlinear effects are often responsible for development of more complex spatial and temporal structure of disturbances as the forcing of the system is increased. Furthermore, the models presented above ignore the complications introduced by phase mixing [51]. This occurs when gradients in background fields lead to frequency (and wavelength) detuning between neighbouring perturbation fields; it is known to have important implications for both Alfvén waves [51] and (magnetically-modified) thermal Rossby waves in a sphere [56, 57]. Although simple linear models are useful for determining the most unstable modes in a

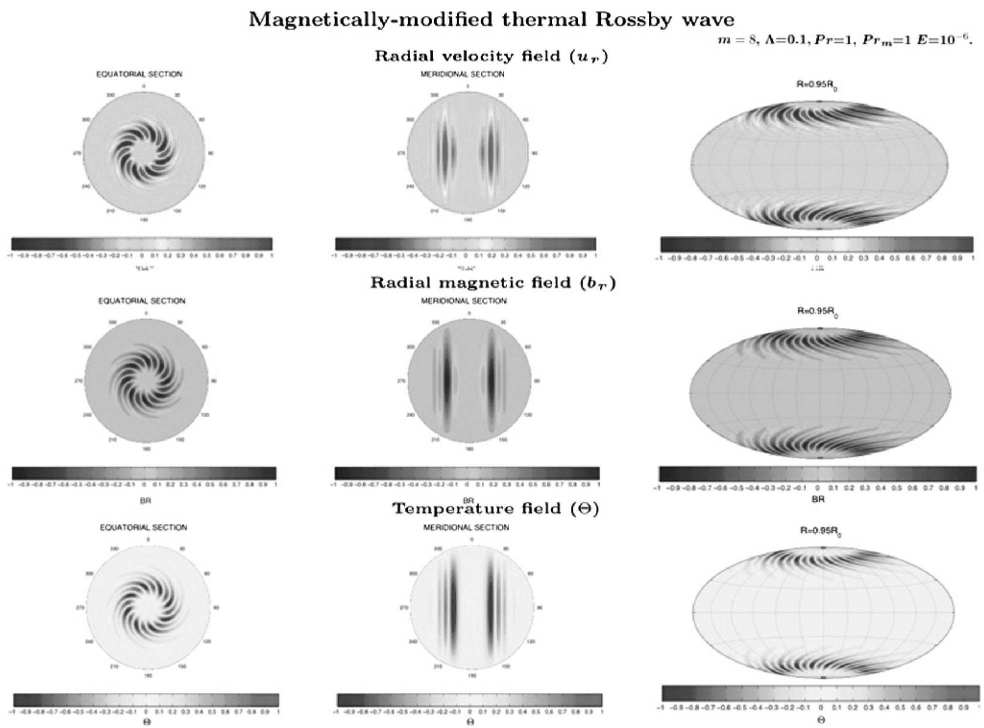

Fig. 4. Example of the structure of a $m = 8$, marginally-critical, magnetically-modified thermal Rossby wave for $E = 10^{-6}$, $Pr = 1$, $Pr_m = 1$, $\Lambda = 0.1$. Top row shows the perturbation radial velocity field, middle row shows the perturbation radial magnetic field and bottom row shows the perturbation temperature field. Left hand column shows a section through the equatorial plane, centre column shows a north-south meridional section, right hand column shows the fields just below the outer boundary. Taken from Finlay (2005) [43].

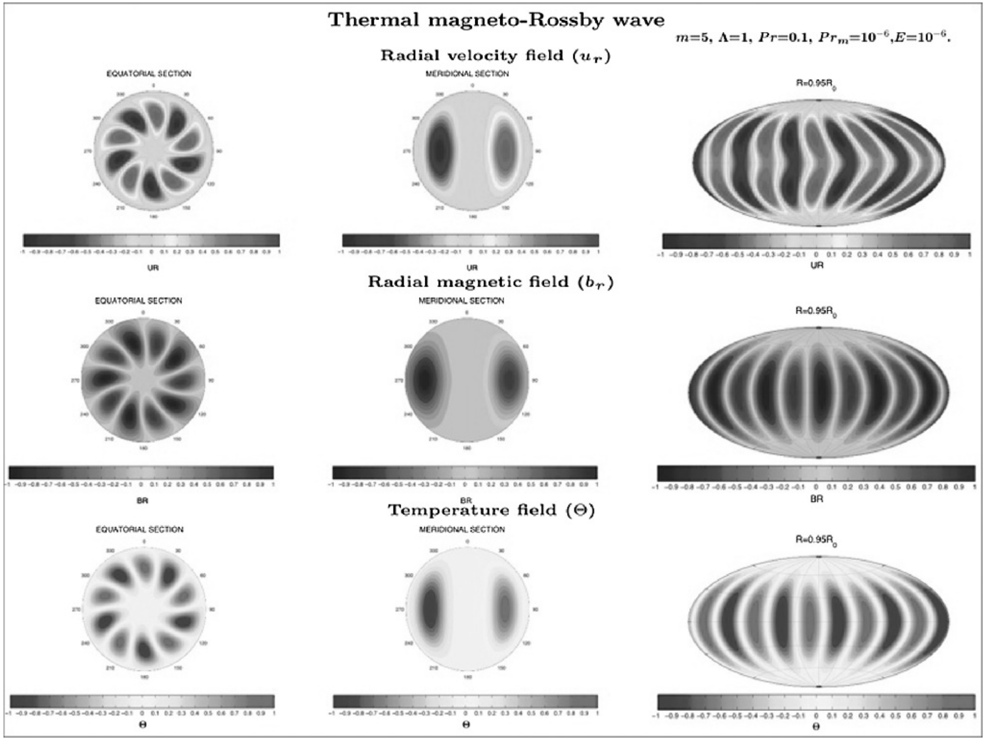

Fig. 5. Example of the structure of a $m = 5$, marginally-critical, thermal magneto- Rossby wave for $E = 10^{-6}$, $Pr = 0.1$, $Pr_m = 10^{-6}$, $\Lambda = 1$. Top row shows the perturbation radial velocity field, middle row shows the perturbation radial magnetic field and bottom row shows the perturbation temperature field. Left hand column shows a section through the equatorial plane, centre column shows a north-south meridional section, right hand column shows the fields just below the outer boundary. Taken from Finlay (2005) [43].

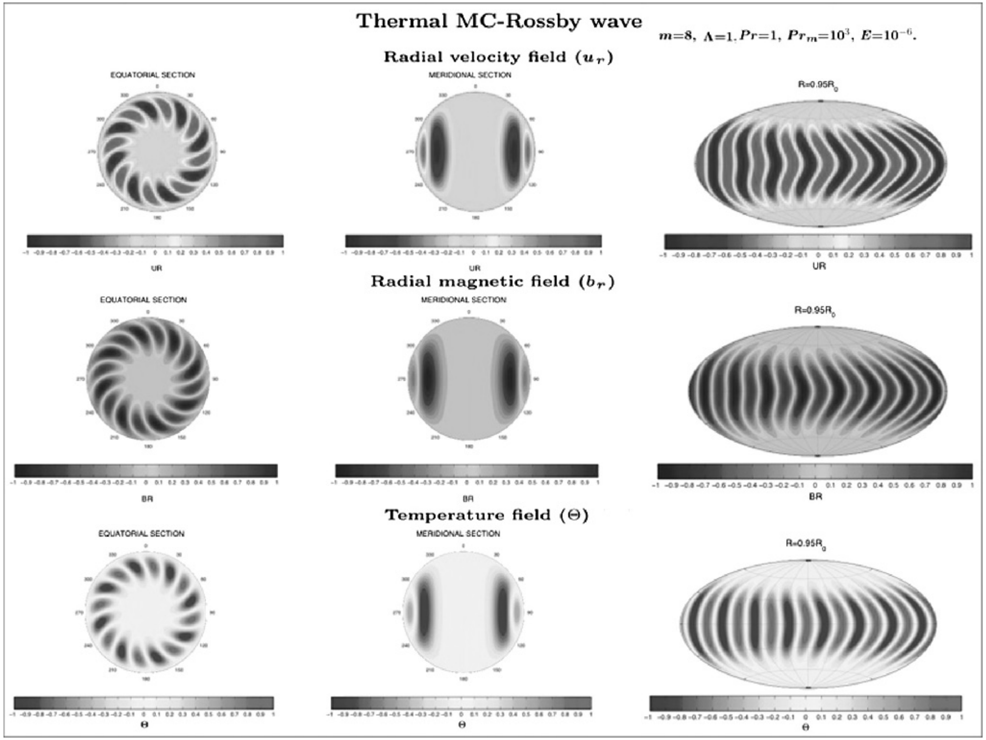

Fig. 6. Example of the structure of a $m = 8$, marginally critical, thermal MC Rossby wave $E = 10^{-6}$, $Pr = 1$, $Pr_m = 10^3$, $\Lambda = 1$. Top row shows the perturbation radial velocity field, middle row shows the perturbation radial magnetic field and bottom row shows the perturbation temperature field. Left hand column shows a section through the equatorial plane, centre column shows a north-south meridional section, right hand column shows the fields just below the outer boundary. Taken from Finlay (2005) [43].

particular parameter regime, the neglect of nonlinear processes and gradients in background fields makes detailed comparisons of model results with geophysical and astrophysical observations a perilous activity.

Some limited progress has been made on developing more sophisticated nonlinear models. Roberts and Stewartson [83] performed a weakly nonlinear analysis of MAC waves in a plane layer geometry. Eltayeb and co-workers [26, 30] derived equations for diffusionless MAC waves in a plane layer with a slowly varying background mean state. Their equations describe the evolution of the wave amplitude via the conservation of wave action (wave energy divided by wave frequency per unit volume). Ewen and Soward [31–33] performed a weakly nonlinear analysis of a QG cylindrical annulus model of MAC waves. They derived and analysed equations describing the amplitude modulation of thermal magneto-Rossby waves, finding that a geostrophic flow is driven nonlinearly by the Lorentz forces resulting from magnetic field perturbations, and is linearly damped by the Ekman boundary layer. They also found that the nonlinear interaction resulting from the geostrophic flow can redistribute energy amongst wave modes. Cardin and Olson [19] used the QG approximation to numerically simulate fully non-linear magnetoconvection and found that imposing a strong magnetic field reduced the observed wavenumber and reduced the amplitude of zonal flows driven by nonlinear Reynolds stresses.

In full spherical geometry Walker and Barenghi [100] considering only the leading order nonlinearity of the geostrophic flow found that the resulting flow strongly influenced the frequency and propagation direction of waves. Zhang [104] studied nonlinear rotating magnetoconvection in a spherical shell. He found a nonlinear bifurcation occurred as the Rayleigh number was increased, that involved simultaneous breaking of temporal and azimuthal symmetry leading to vacillating wave motions.

Theoretical study of nonlinear waves in rapidly-rotating, electrically conducting fluids in the presence of strong magnetic fields is still in its infancy. In particular efforts have focused on convection-driven systems to the neglect of other possible driving mechanisms such as elliptical instabilities, shear instabilities, boundary layer instabilities and magnetic instabilities. Future investigations into these possibilities will likely yield important insights enabling better comparisons with observations.

8. Waves in experiments

Having reviewed the properties of waves in the presence of magnetic fields, rotation and convection using a range of theoretical models, in this section a link is made to physical reality in the form of laboratory experiments.

Alfvén waves were first studied experimentally in liquid mercury by Lundquist [69] and in liquid sodium by Lehnert [65]. These studies confirmed the existence of Alfvén waves, but also highlighted the difficulty in studying the simplest plane waves experimentally since at low frequencies their wavelength becomes larger than the apparatus, while at high frequencies the inertia of the liquid destroys ideal behaviour. Most recent experimental work on Alfvén waves has focused on plasmas rather than liquid metals.

Inertial waves have been more intensively studied experimentally. It is likely that Kelvin himself first observed them in a public demonstration [59]. Interest in the late 20th century was stimulated by the beautiful study of Schultz [46] and by the photographs shown in the monograph of Greenspan [49]. Much recent work has focused on how Inertial waves might be generated by elliptical instability, for example by tidal straining or precessional forcing (see the studies by Aldridge and co-workers [4, 91] and LeGal and co-workers [25, 62, 63]) and on the nonlinear interactions and evolution of Inertial waves, for example leading to the phenomenon of resonant growth and collapse cycles [62, 71, 72]. In general, when viscous corrections and appropriate boundary conditions are employed, the predictions of linear theory for inertial wave frequencies, wavenumbers and growth rates have proved spectacularly successful.

In contrast to the numerous studies of Alfvén and Inertial waves, there have been only a very small number of studies of wave motions in rapidly-rotating electrically conducting fluids in the presence of magnetic fields. Lacaze et al. [64] have studied the induction produced by Inertial waves in a Galinstan cylinder in the presence of a weak axial magnetic field. Kelley et al. [60] have identified the induction signature of Inertial waves in a liquid sodium spherical Couette experiment with an applied axial magnetic field. In both cases, the Lorentz force was not strongly influencing the dynamics, and the magnetic field was simply acting as a tracer for the Inertial waves. In contrast the DTS experiment at Grenoble [20, 75], also a spherical Couette experiment using liquid sodium, is designed to operate in a regime where the Lorentz force constitutes an important part of the leading order force balance. Preliminary results show non-axisymmetric motions in this experiment to be dominated by wave motions [90]. It seems likely that these must are some form of MC wave, but the analysis is complicated by the coincidence of timescales (magnetic diffusion, Alfvén and inertial) in the experiment, the non-uniform imposed magnetic field and the difficulty in imaging the interior flow of the liquid metal. Nonetheless, this challenging experiment is very exciting as it opens up a new avenue for experimental tests of MC wave theory that promises many further surprises.

At this time, few experiments on MAC waves have yet been reported. Experiments on rotating magnetoconvection in a weak applied field have recently been reported by Gillet et al. [48]. The rotating magnetoconvection experiment at UCLA of Aurnou, King and co-workers promises to approach the interesting regime where the Lorentz forces play a leading role in the dynamics and heat transport.

Many possibilities exist for future experiments probing waves in the presence of magnetic fields, rotation and convection. For example, it would be particularly interesting to build a simple experiment (e.g. with cylindrical geometry and uniform applied magnetic field parallel to the rotation axis) designed to obtain a clear splitting of fast and slow MC modes. This would allow the intruiging slow MC mode to be isolated so its properties might be studied in detail. At the moment it is a significant engineering challenge to produce splitting of MC modes due to the large rotation rates required, but such technical issues are not insurmountable.

9. Waves in numerical dynamo simulations

One of the most powerful tools for understanding the dynamics of geophysical and astrophysical systems is full numerical simulation of the governing (MHD) equations. Although currently limited in the regions of parameter space in which they can accurately operate, such simulations are capable of capturing important aspects of solar and (especially) terrestrial magnetic field generation and evolution.

Since they solve the full rotating MHD equations (i.e. the induction equation and Navier-Stokes equation including Coriolis, Lorentz and full non-linear inertial terms), and typically drive motions via thermal convection, these simulations can in principle capture Alfvén, inertial, MC and MAC waves. In fact, such waves are often viewed as a nuisance by modellers since they place tight requirements on time-steps necessary to capture the dynamics [54,99]. However, in present simulations the influence of diffusion (especially viscous and thermal diffusion) is stronger than in true geophysical and astrophysical systems due to computational constraints. As a consequence many potentially interesting waves are often over damped and are not able to be studied.

Nonetheless, a few preliminary studies suggest that simulations are beginning to reach the regimes where they can provide interesting information concerning waves. Glatzmaier has reported 2D simulations of magnetoconvection where Alfvén waves are clearly evident, while Dumberry [24] and Wicht have independently studied the special case of geostrophic Alfvén waves (Torsional Oscillations) in fully 3D geodynamo simulations. In my Ph.D. thesis [43], I showed that in a rather simple 3D, convection-driven, dynamo with Rayleigh number only 3 times critical, thermally-driven magneto-Rossby waves modes of convection could be identified. In simulations with more realistic parameters (lower Ekman number and more super-critical Rayleigh number) more localised wave-like features were found in both the velocity field and the magnetic field close to the outer boundary.

Investigations of waves in dynamo simulations with diffusivities as small as possible, including detailed study of the evolution of the force balance involved in wave-like features, certainly seems to be a fruitful direction for future research. The detailed diagnostics provided by simulations should allow many hypotheses concerning wave motions and their nonlinear evolution to be tested. One of the biggest and most important questions that simulations can answer is what role MC/MAC waves play when the magnetic field structure is not uniform, but is dominated by compact regions of strong magnetic field where dynamo action occurs. There Lorentz forces will be particularly dominant and phase mixing of waves is likely to occur. Such questions cannot be answered by simple linear theories with uniform applied fields such as those presented in previous sections.

10. Concluding remarks on waves in geophysical and astrophysical systems

In these lecture notes, I have reviewed the theory of waves in the presence of magnetic fields, rotation and convection and discussed how experiments and numerical simulations are becoming important tools for furthering our understanding of these phenomena.

Are the waves discussed above of geophysical and astrophysical interest? Since these systems often possess magnetic fields and undergo rapid rotation they are certainly likely to support waves. Furthermore, they are usually characterized by large hydrodynamic and hydromagnetic Reynolds numbers resulting from weak viscous and magnetic diffusivities, so it seems plausible that waves will not be damped too rapidly in these systems. The key question is therefore whether mechanisms exist for exciting such hydromagnetic waves.

Personally, I find it is hard to imagine how waves could not be important in many geophysical and astrophysical fluid systems, because they are the natural response of a hydromagnetic system to perturbation. For example, turbulent convection could continuously excite a very broadband spectrum of waves, similar to the scenario for the driving helioseismic waves on the sun. Moreover, waves are the natural manifestation of a variety of instability mechanisms including convective instability [9], magnetic instability [1], shear instability [39], boundary layer instability [23] topographical forcing [52] and elliptical (tidal or precessional) instability [61]. Which (if any) of these mechanisms are relevant depends on the details of the particular system being studied.

In astrophysical systems involving plasmas or giant gaseous planets, compressibility effects will not be negligible and the theory outlined above will have to be modified accordingly. Nonetheless, there is already considerable astrophysical interest in waves similar to those discussed above, for example regarding the role hydromagnetic waves might play in the dynamics of the tachocline [89]. Considering planetary cores (including that of the Earth), incompressibility is likely to be a reasonable first approximation, and observations of geomagnetic field evolution [42] provide intruiging evidence in favour of the existence of wave-like features. Thermally-driven magneto-Rossby waves advected by background zonal flows or topographically-driven MC waves appear the most likely candidates for explaining the geophysical observations [43]. It is presently unclear whether elliptical instability could occur in Earth's core [61] or whether it could excite slow MC/MAC waves.

Though the basic theory of waves in the presence of magnetic fields, rotation and convection exists, much remains to be done in order to apply it to geophysical and astrophysical systems. The input from experimental studies in coming years together with development of nonlinear theories of wave-wave and wave-mean flow interactions informed by study of waves in numerical simulations, are likely to be crucial in the future development of the subject.

Acknowledgements

I would like to express my gratitude to Philippe Cardin and the scientific committee for organizing the 'Dynamos' summer school and to thank the principal lecturers for their efforts in delivering informative and thought-provoking lectures. I am also happy to acknowledge stimulating conversations regarding waves with my fellow students, particularly with Doug Kelley, Wietze Herreman and Mathieu Dumberry. Thanks also to Nadège Gagniere for reading and commenting on these notes.

Appendix A. Hide's β-plane model of MC Rossby waves

Hide [52] developed a simple analytical model for MC waves in a spherical shell geometry. He assumed that the waves would have a two dimensional form, being to a first approximation invariant parallel to the rotation axis. He was therefore able to focus on local motions of fluid columns in the eastward $\hat{\boldsymbol{x}}$ and northward $\hat{\boldsymbol{y}}$ directions in spherical geometry and focused on the evolution of the vertical $\hat{\boldsymbol{z}}$ component of vorticity. He followed Rossby [88] and assumed that the Coriolis force could be approximated as varying linearly in the north-south direction at a fixed latitude. This results in the a simplification of the Coriolis force to the form $-fu_y$ in the eastward direction and fu_x in the northward direction, where $f_c = 2\Omega \sin\theta_{lat} + \frac{2\Omega\cos\theta_{lat}}{c} y = f_0 + \beta y$ and c is the outer radius of the spherical shell. Though $\beta = \frac{2\Omega\cos\theta_{lat}}{c}$ in thin spherical shell, Hide argued that it should take the opposite sign $\left(\beta = -\frac{2\Omega\cos\theta_{lat}}{c}\right)$ in thick spherical shells.

Hide studied a scenario where the imposed magnetic field $\boldsymbol{B_0}$ was uniform but inclined at an arbitrary angle to the eastward direction; here I present his model for a special case when $\boldsymbol{B_0}$ is purely eastwards. The background velocity field is also assumed to be zero for simplicity. Magnetic and viscous diffusion and all thermal and density stratification effects are also neglected. The linearized equations governing the evolution of the velocity field and magnetic field disturbances $(\boldsymbol{u}, \boldsymbol{b})$ on the β-plane, after the subtraction of the leading order geostrophic balance between pressure and the constant part of the Coriolis force ($f_0 = 2\Omega\sin\theta_{lat}$), are then

$$\frac{\partial u_x}{\partial t} - \beta y u_y = -\frac{1}{\rho_0}\frac{\partial p}{\partial x}, \tag{A.1}$$

$$\frac{\partial u_y}{\partial t} + \beta y\, u_x = -\frac{1}{\rho_0}\frac{\partial p}{\partial y} + \frac{B_0}{\rho_0\mu_0}\left(\frac{\partial b_y}{\partial x} - \frac{\partial b_x}{\partial y}\right), \tag{A.2}$$

$$\frac{\partial b_x}{\partial t} = B_0\frac{\partial u_x}{\partial x}, \tag{A.3}$$

$$\frac{\partial b_y}{\partial t} = B_0\frac{\partial u_y}{\partial x}, \tag{A.4}$$

where B_0 is the strength of the background magnetic field. Note for this special case of $\boldsymbol{B_0} = B_0\widehat{\boldsymbol{x}}$ there is no Lorentz force term in (A.1).

Taking the curl of the momentum equations ($\frac{\partial}{\partial y}$ of (A.1) minus $\frac{\partial}{\partial x}$ of (A.2)) yields the $\widehat{\boldsymbol{z}}$ component of the vorticity equation

$$\frac{\partial \zeta}{\partial t} + \beta u_y = \frac{B_0}{\rho_0\mu_0}\frac{\partial}{\partial x}\left(\frac{\partial b_y}{\partial x} - \frac{\partial b_x}{\partial y}\right), \tag{A.5}$$

where $\zeta = \left(\frac{\partial u_x}{\partial y} - \frac{\partial u_y}{\partial x}\right)$ is the z component of vorticity. Taking the time derivative of (A.5), substituting from $\frac{\partial}{\partial y}$ (A.3) and $\frac{\partial}{\partial x}$ (A.4) and operating with $\nabla_H^2 = \left(\frac{\partial}{\partial x^2} + \frac{\partial}{\partial y^2}\right)$ to eliminate u_y, an equation for the evolution of ζ on the β plane is obtained

$$\left(\frac{\partial^2}{\partial t^2} - \frac{B_0^2}{\rho_0\mu_0}\frac{\partial^2}{\partial x^2}\right)\nabla_H^2\zeta + \beta\frac{\partial}{\partial t}\left(\frac{\partial \zeta}{\partial x}\right) = 0. \tag{A.6}$$

Plane wave solutions of the form $\zeta = \hat{\zeta}e^{i(kx+ky-\omega t)}$, where k is the wavenumber of the disturbance (for simplicity assumed to be the same in the northward and eastward directions), and ω is the angular frequency of the waves, can now be considered. Substituting the plane wave solutions into (A.6) yields the dispersion relation

$$\omega^2 + \frac{\beta\omega}{k} - \frac{B_0^2 k^2}{\rho_0 \mu_0} = 0. \tag{A.7}$$

This quadratic equation can be solved to give an expression for ω in terms of k,

$$\omega = -\frac{\beta}{2k} \pm \frac{\beta}{2k}\left(1 + \frac{4B_0^2 k^4}{\rho_0 \mu_0 \beta^2}\right)^{1/2}. \tag{A.8}$$

For long wavelength disturbances in a rapidly-rotating fluid $\left(\frac{4B_0 k^4}{\rho_0\mu_0\beta^2}\right)$ will be small and a Taylor expansion in this parameter shows that two rather different solutions for ω are possible to leading order

$$\omega_r = -\frac{\beta}{k} \quad \text{and} \quad \omega_m = \frac{B_0^2 k^3}{\mu_0 \rho_0 \beta}. \tag{A.9}$$

The mode ω_r is recognizable as a Rossby wave on a β-plane [49, 88]. Rossby waves are the special low-frequency, columnar, uni-directional inertial waves that arise because of the latitudinal variation of the Coriolis force in spherical shell. ω_m on the other hand corresponds to a wave very similar in form to the slow MC wave found in a rotating plane layer, but inversely proportional to $\beta = \frac{2\Omega\cos\theta_{lat}}{c}$ rather than 2Ω. It is often referred to as a (slow) MC Rossby wave or sometimes as Hide's wave. Note that if the wavenumbers in the $\widehat{\boldsymbol{x}}$ and $\widehat{\boldsymbol{y}}$ directions are different then slightly more complicated dispersion relations are obtained, but the essential physics remains the same.

Appendix B. Malkus' model of MC waves in a full sphere

Malkus [70] analytically studied MC waves in a full sphere geometry using a special toroidal and purely azimuthal imposed magnetic field of the form $\boldsymbol{B_0} = B_0 r \sin\theta\, \widehat{\boldsymbol{\phi}}$ where $0 \le r \le 1$. Here, $r = r'/c$ with r' being the dimensional spherical polar radius, c is the dimensional radius of the outer spherical boundary, θ is the co-latitude, and B_0 is the maximum magnitude of the imposed field at the outer boundary in the equatorial plane. This field (often called the Malkus field) is invariant on cylindrical surfaces aligned with the rotation axis and increases in strength linearly with distance from the rotation axis. It can be conveniently written in cylindrical polar co-ordinates as $\boldsymbol{B_0} = B_0 s\, \widehat{\boldsymbol{\phi}}$ where $0 \le s \le 1$ where s is the normalized cylindrical radius. It is also force free (i.e. $\nabla \times (\nabla \times \boldsymbol{B_0}) = 0$), so $\boldsymbol{U}_0 = 0$ is a consistent choice for the co-existing background velocity field.

Defining the rotation axis to be along $\hat{\boldsymbol{z}}$ and working in cylindrical polar coordinates $(\hat{\boldsymbol{s}}, \hat{\boldsymbol{z}}, \hat{\boldsymbol{\phi}})$, the linearized governing equations for the velocity and magnetic field perturbations ignoring density stratification and all diffusive processes are

$$\rho_0 \frac{\partial \boldsymbol{u}}{\partial t} + 2\rho_0 \Omega (\hat{\boldsymbol{z}} \times \boldsymbol{u}) = -\nabla p + \frac{1}{\mu_0} \left[(\boldsymbol{B_0} \cdot \nabla)\boldsymbol{b} + (\boldsymbol{b} \cdot \nabla)\boldsymbol{B_0} \right], \tag{B.1}$$

$$\frac{\partial \boldsymbol{b}}{\partial t} = \nabla \times (\boldsymbol{u} \times \boldsymbol{B_0}). \tag{B.2}$$

The major difference of the Malkus model compared to studies of uniform imposed magnetic fields is in the inclusion of the final term in the momentum equation $(\boldsymbol{b} \cdot \nabla)\boldsymbol{B_0}$ resulting from the non-zero spatial gradient in $\boldsymbol{B_0}$.

For the Malkus field, the Lorentz force and the advection term in the induction equation take very simple forms. Recognizing that the advection term can be rewritten as $\nabla \times (\boldsymbol{u} \times \boldsymbol{B_0}) = (\boldsymbol{B_0} \cdot \nabla)\boldsymbol{u} - (\boldsymbol{u} \cdot \nabla)\boldsymbol{B_0}$ and making use of the following relations that hold for the Malkus field

$$(\boldsymbol{b} \cdot \nabla)\boldsymbol{B_0} = B_0 (\hat{\boldsymbol{z}} \times \boldsymbol{b}), \tag{B.3}$$

$$(\boldsymbol{B_0} \cdot \nabla)\boldsymbol{b} = B_0 \left(\frac{\partial \boldsymbol{b}}{\partial \phi} + \hat{\boldsymbol{z}} \times \boldsymbol{b} \right), \tag{B.4}$$

$$(\boldsymbol{B_0} \cdot \nabla)\boldsymbol{u} = B_0 \left(\frac{\partial \boldsymbol{u}}{\partial \phi} + \hat{\boldsymbol{z}} \times \boldsymbol{u} \right), \tag{B.5}$$

$$(\boldsymbol{u} \cdot \nabla)\boldsymbol{B_0} = B_0 (\hat{\boldsymbol{z}} \times \boldsymbol{u}) \tag{B.6}$$

the governing equations become

$$\rho_0 \frac{\partial \boldsymbol{u}}{\partial t} + 2\rho_0 \Omega (\hat{\boldsymbol{z}} \times \boldsymbol{u}) = -\nabla p + \frac{B_0}{\mu_0} \left[\frac{\partial \boldsymbol{b}}{\partial \phi} + 2\hat{\boldsymbol{z}} \times \boldsymbol{b} \right], \tag{B.7}$$

$$\frac{\partial \boldsymbol{b}}{\partial t} = B_0 \left(\frac{\partial \boldsymbol{u}}{\partial \phi} \right). \tag{B.8}$$

Substituting in azimuthally travelling wave solutions of the form

$$(\boldsymbol{u}, \boldsymbol{b}) = (\hat{\boldsymbol{u}}(s,z) e^{i(m\phi - \omega t)}, \hat{\boldsymbol{b}}(s,z) e^{i(m\phi - \omega t)}), \tag{B.9}$$

where m is the azimuthal wavenumber of the wave, and ω is its angular frequency leads to the relations

$$-i\omega\rho_0 \boldsymbol{u} + 2\omega\rho_0 (\hat{\boldsymbol{z}} \times \boldsymbol{u}) = -\nabla p + \frac{B_0}{\mu} \left(im\boldsymbol{b} + 2(\hat{\boldsymbol{z}} \times \boldsymbol{b}) \right), \tag{B.10}$$

$$-i\omega \boldsymbol{b} = imB_0 \boldsymbol{u}. \tag{B.11}$$

Substituting from (B.11) into (B.10) for $\boldsymbol{b}$ and collecting like terms yields a single equation

$$\mathcal{L}_1(\widehat{\boldsymbol{z}} \times \boldsymbol{u}) + \mathcal{L}_2\boldsymbol{u} + \nabla p = 0, \tag{B.12}$$

where

$$\mathcal{L}_1 = 2\left(\Omega\rho_0 + \frac{B_0^2 m}{\mu_0\omega}\right), \qquad \mathcal{L}_2 = \left(-i\omega\rho_0 + i\frac{B_0^2 m^2}{\mu_0\omega}\right). \tag{B.13}$$

This has the same form as the momentum equation governing the evolution of Inertial waves in a sphere [73, 102, 108], but with $\mathcal{L}_2$ rather than $-i\omega\rho_0$ and $\mathcal{L}_1$ rather than $2\rho_0\Omega$. The consequence of the presence of the Malkus background magnetic field is therefore only that the strength of the latitude-dependent Coriolis force and the timescale of the inertial response of the fluid have been changed.

(B.12) can be re-written in terms of pressure only (for details of this manipulation consult [70]) as

$$\left(\mathcal{L}_2^2\nabla^2 + \mathcal{L}_1^2\frac{\partial}{\partial z}\right) p = 0. \tag{B.14}$$

The appropriate rigid spherical boundary condition ($\boldsymbol{u} \cdot \hat{\boldsymbol{n}} = 0|_{r=c}$ where $\hat{\boldsymbol{n}}$ is a normal to the spherical surface), in a form applicable to pressure can be obtained using the link between $\boldsymbol{u}$ and p in (B.12) and turns out to be

$$\left(\mathcal{L}_2^2 s\frac{\partial}{\partial s} + (\mathcal{L}_1^2 + \mathcal{L}_2^2)z\frac{\partial}{\partial z} + i\mathcal{L}_1\mathcal{L}_2\right) p = 0. \tag{B.15}$$

Next, by choosing

$$\lambda_{in} = \frac{2\mathcal{L}_2}{i\mathcal{L}_1} \quad \text{so that } -\lambda_{in}^2 = \frac{4\mathcal{L}_2^2}{\mathcal{L}_1^2} \tag{B.16}$$

the governing equations in p are transformed into the standard form of the Poincaré equation for Inertial waves in a sphere (see, for example, [102])

$$\left(\nabla^2 - \frac{4}{\lambda_{in}^2}\frac{\partial}{\partial z}\right) p = 0, \tag{B.17}$$

and the associated boundary condition

$$\left(s\frac{\partial}{\partial s} + \frac{2m}{\lambda_{in}} - \frac{4}{\lambda_{in}^2}z\frac{\partial}{\partial z}\right) p = 0 \quad \text{on } s^2 + z^2 = 1. \tag{B.18}$$

The solution to the Inertial wave problem in the sphere involves finding eigenvalues λ_{in} and associated eigenvectors which satisfy (B.17) and (B.18). The solutions are very complicated in general and have only recently been written down explicitly by Zhang and co-workers [108], though Malkus [70] and Zhang [102] had earlier studied some simple cases.

Regarding λ_{in} as known, the angular frequencies ω of the solutions to the hydromagnetic wave problem in a sphere in the presence of the Malkus magnetic field are now defined. By substituting expressions for $\mathcal{L}_1$, $\mathcal{L}_2$ into (B.16) the relation between λ_{in} and ω is found to be

$$\lambda_{in} = \frac{2\left(-\omega\rho_0 + \frac{B_0^2 m^2}{\mu_0 \omega}\right)}{2\left(\Omega\rho_0 + \frac{B_0^2 m}{\mu_0 \omega}\right)}, \tag{B.19}$$

which can be rearranged into a quadratic equation in the hydromagnetic wave angular frequency ω

$$\omega^2 + \Omega\lambda_{in}\omega + \frac{B_0^2 m}{\rho_0\mu_0}(\lambda_{in} - m) = 0, \tag{B.20}$$

that has solutions

$$\omega = \frac{\Omega\lambda_{in}}{2}\left[-1 \pm \left(1 - \frac{4B_0^2 m(\lambda_{in} - m)}{\Omega^2\lambda_{in}^2\rho_0\mu_0}\right)^{1/2}\right]. \tag{B.21}$$

In the case of large wavelength disturbances (small m) and rapid rotation, when $\frac{4B_0^2 m}{\Omega^2\lambda_{in}^2\rho_0\mu_0}$ is small, a Taylor series expansion shows that the two possible solutions are to leading order [70]

$$\omega_i \sim -\Omega\lambda_{in} \quad \text{and} \quad \omega_m \sim \frac{B_0^2}{\Omega\rho_0\mu_0}\frac{m(m - \lambda_{in})}{\lambda_{in}}. \tag{B.22}$$

ω_i is essentially an Inertial wave, that can travel both eastward and westward depending on the sign of λ_{in}, while ω_m is a slow MC wave where the inertial term is unimportant and the Lorentz and Coriolis forces balance each other to leading order.

The relation between Malkus' slow MC wave and Hide's slow MC-Rossby waves becomes clear if one considers a λ_{in} corresponding to a quasi-geostrophic Inertial wave (QGIW) [17, 105, 108]. Such QGIWs are unidirectional (always travel eastward because λ_{in} is < 0 in a full sphere), and columnar in structure parallel to the rotation axis: they are in fact none other than Rossby waves in a sphere. For such QGIWs with $\lambda_{in} < 0$, the associated slow MC waves (i.e. the MC-Rossby wave) will travel westward as predicted by Hide's analysis.

The ingenious analysis of Malkus, based around a clever choice of imposed field, thus permits the hydromagnetic wave problem in the full sphere to reduce to the classic problem of Inertial waves in a full sphere. It should however be remembered that the Malkus field is rather atypical in its cylindrical symmetry. In general the effect of the Lorentz forces from magnetic fields will not be able to be absorbed completely into modified Coriolis and inertial terms.

Appendix C. Busse and Soward's QG model of MAC waves

Busse [14] and Soward [93] developed a formally precise quasi-geostrophic (QG) model of 2D (structurally invariant parallel to the rotation axis), thermally-driven MAC waves. In a cylindrical annulus with sloping upper and lower boundaries, a uniform azimuthal magnetic field is imposed together with a cylindrically radial background temperature gradient and gravity field that combine to give a cylindrically radial buoyancy force (see Fig. 3). The gap D between the inner and outer cylinders is assumed to be small compared to the height of the annulus L, making it possible to work in a local Cartesian co-ordinate system. In this scenario it is possible to write $\widehat{\boldsymbol{\Omega}} = \widehat{\boldsymbol{z}}$, $\widehat{\boldsymbol{g}} = -\widehat{\boldsymbol{x}}$ and $\widehat{\nabla T_0} = -\widehat{\boldsymbol{x}}$ so that $(\boldsymbol{u} \cdot \nabla) T_0 = -\beta' u_x$ while $\boldsymbol{B_0} = B_0 \widehat{\boldsymbol{y}}$ so $(\boldsymbol{b} \cdot \nabla)\widehat{\boldsymbol{B_0}} = 0$, $(\widehat{\boldsymbol{B_0}} \cdot \nabla)\boldsymbol{b} = \frac{\partial \mathbf{b}}{\partial y}$ and $\nabla \times (\boldsymbol{u} \times \widehat{\boldsymbol{B_0}}) = \frac{\partial \mathbf{u}}{\partial y}$. With these simplifications the linearized momentum, induction and heat transport equations governing the evolution the velocity, magnetic and temperature field can be written as,

$$E\left(\frac{\partial}{\partial t} - \nabla^2\right)\boldsymbol{u} + (\widehat{\boldsymbol{z}} \times \boldsymbol{u}) = -\nabla p + E Ra \Theta \widehat{\boldsymbol{x}} + \Lambda \frac{\partial \boldsymbol{b}}{\partial y}, \tag{C.1}$$

$$\left(\nabla^2 - Pr_m \frac{\partial}{\partial t}\right)\boldsymbol{b} = \frac{\partial \boldsymbol{u}}{\partial y}, \tag{C.2}$$

$$\left(\nabla^2 - Pr \frac{\partial}{\partial t}\right)\Theta = u_x, \tag{C.3}$$

where maximum height of the annulus L has been used as the unit of length and the viscous diffusion time has been used as the unit of time. The non-dimensional control parameters and their physical meanings are defined in (6.2) to (6.6) in the main text.

Taking the $\widehat{\boldsymbol{z}}$ component of the curl of (C.1) and (C.2) while defining the axial component of perturbation vorticity as $\zeta = \widehat{\boldsymbol{z}} \cdot (\nabla \times \boldsymbol{u})$ and the axial component of the perturbation electric current density as $j = \widehat{\boldsymbol{z}} \cdot (\nabla \times \boldsymbol{b})$ gives

$$E\left(\frac{\partial}{\partial t} - \nabla^2\right)\zeta + \frac{\partial u_z}{\partial z} = -ERa\frac{\partial \Theta}{\partial y} + \Lambda\frac{\partial j}{\partial y}, \tag{C.4}$$

$$\left(\nabla^2 - Pr_m\frac{\partial}{\partial t}\right) j = \frac{\partial \zeta}{\partial y}. \tag{C.5}$$

The assumption of quasi-geostrophy is next implemented by first integrating equations (C.4), (C.5) and (C.3) with respect to z and dividing by the depth of the fluid. ζ, j, and Θ can then be interpreted as the vertically averaged perturbations in axial vorticity, axial electrical current and temperature respectively. This is reasonable because geostrophy (z independence) holds to leading order when the slope of the top boundary is small (see, for example, [16] for a formal development of the QG model and [15] for a discussion of its utility). However, because of the presence of the sloping top and bottom boundaries, the term $\frac{\partial u_z}{\partial z}$ arising from the Coriolis force cannot be z independent if mass is conserved. Conservation of mass for the incompressible fluid ($\nabla \cdot \boldsymbol{u} = 0$) applied at the boundary requires that[4]

$$\int_0^1 \frac{\partial u_z}{\partial z} dz = [u_z]_0^1 = -\beta^* u_x, \tag{C.6}$$

where the non-dimensional parameter β^* is the tangent of the angle between the boundary slope and the equatorial plane, and is related to the dimensional β-plane parameter appearing in Hide's model (see Appendix A) by $\beta = 2\Omega\beta^*/L$. To leading order, the velocity fields in the QG approximation are 2D so they can be represented by a stream function χ where $u_x = \frac{\partial \chi}{\partial y}$ and $u_y = -\frac{\partial \chi}{\partial x}$ so the $\widehat{\boldsymbol{z}}$ component of vorticity is $\zeta = -\nabla \chi$. The governing equations for the QG system in terms of χ, j and Θ are then,

$$-E\left(\frac{\partial}{\partial t} - \nabla^2\right)\nabla^2\chi + \beta^*\frac{\partial \chi}{\partial y} = -ERa\frac{\partial \Theta}{\partial y} + \Lambda\frac{\partial j}{\partial y}, \tag{C.7}$$

$$\left(\nabla^2 - Pr\frac{\partial}{\partial t}\right)\Theta = -\frac{\partial \chi}{\partial y}, \tag{C.8}$$

$$\left(\nabla^2 - Pr_m\frac{\partial}{\partial t}\right) j = -\frac{\partial}{\partial y}\nabla^2\chi. \tag{C.9}$$

[4]This expression ignores the influence of viscous boundary layers and associated Ekman pumping. It only rigorously applies when free slip boundary conditions are implemented.

Plane wave solutions for χ, j and Θ proportional to $e^{i(kx+ky-\omega t)}$ (invariant in the $\hat{z}$ direction and taking k to be an estimate of the wavenumber in both the x and y directions for simplicity) can then be substituted into (C.7) to (C.9). This yield relations between j and χ, and between Θ and χ

$$\Theta = \frac{-ik\chi}{-k^2 + iPr\omega} \quad \text{and} \quad j = \frac{ik^3\chi}{-k^2 + iPr_m\,\omega}, \tag{C.10}$$

which when substituted into (C.7) give a dispersion relation for the complex frequency ω

$$E(-i\omega + k^2) + \frac{i\beta^*}{k} = \frac{ERa}{-iPr\,\omega + k^2} - \frac{\Lambda k^2}{-iPr_m\omega + k^2}. \tag{C.11}$$

This is the QG dispersion relation discussed in the main text that describes various types of 2D, thermally-driven, Rossby and MC/MAC waves.

References

[1] D.J. Acheson, J. Fluid. Mech. **52**, 529 (1972).

[2] D.J. Acheson, J. Fluid. Mech. **96**, 723 (1980).

[3] D.J. Acheson and R. Hide, Rep. Prog. Physics **36**, 159 (1973).

[4] K. Aldridge, B. Seyed-Mahmoud, G. Henderson and W. Van Wijngaarden, Phys. Earth Plan. Int. **103**, 365 (1997).

[5] H. Alfvén, Nature **150**, 405 (1942).

[6] H. Alfvén and C.-G. Fälthammer, *Cosmical Electrodynamics*, Oxford University Press, 1963.

[7] G.K. Batchelor, *An Introduction to Fluid Mechanics*, Cambridge University Press, 1967.

[8] V. Bjerknes, J. Bjerknes, H. Solberg and T. Bergeron, *Physikalische Hydrodynamik*, Berlin, J. Springer, 1933.

[9] S.I. Braginsky, Geomag. Aeron. (English Translation) **4**, 698 (1964).

[10] S.I. Braginsky, Geomag. Aeron. (English Translation) **7**, 851 (1967).

[11] S.I. Braginsky, in Encycl. Solid. Earth. Geophys. (1989).

[12] G.H. Bryan, Phil. Trans. Roy. Soc. Lond. A. **180**, 187 (1889).

[13] F.H. Busse, J. Fluid Mech. **44**, 441 (1970).

[14] F.H. Busse, Phys. Earth. Planet. Int. **12**, 350 (1976).

[15] F.H. Busse, Phys. Fluids **14**, 1301 (2002).

[16] F.H. Busse and A.C. Or, J. Fluid Mech. **166**, 173 (1986).

[17] F.H. Busse, K. Zhang and X. Liao, Astrophys. J. **631**, L171 (2005).

[18] M.E. Cartan, Bull. Sci. Math. **46**, 317 (1922).

[19] P. Cardin and P. Olson, Earth. Planet. Sci. Lett. **132**, 167 (1995).

[20] P. Cardin, D. Brito, D. Jault, H.C. Nataf and J.P. Masson, Magnetohydrodynamics **38**, 177 (2002).

[21] S. Chandrasekhar, *Hydrodynamic and Hydromagnetic Stability*, Oxford University Press, 1961.

[22] P.A. Davidson, *An Introduction to Magnetohydrodynamics*, Cambridge University Press, 1978.

[23] B. Desjardins, E. Dormy and E. Grenier, Phys. Earth Plan. Int. **124**, 283 (2001).

[24] M. Dumberry and J. Bloxham, Phys. Earth Plan. Int. **140**, 29 (2003).

[25] C. Eloy, P. Le Gal and S. Le Dizés, J. Fluid. Mech. **476**, 357 (2003).

[26] M. El Sawi and I.A. Eltayeb Quart. App. Math. **34**, 187 (1981).

[27] I.A. Eltayeb and P.H. Roberts, Astrophys. J. **162**, 699 (1970).

[28] I.A. Eltayeb, Proc. Roy. Soc. Lond. A. **353**, 145 (1977).

[29] I.A. Eltayeb, Proc. Roy. Soc. Lond. A. **326**, 229 (1972).

[30] I.A. Eltayeb, Phys. Earth. Planet. Int. **24**, 259 (1981).

[31] S.A. Ewen and A.M. Soward, Geophys. Astrophys. Fluid Dyn. **77**, 209 (1994).

[32] S.A. Ewen and A.M. Soward Geophys. Astrophys. Fluid Dyn. **77**, 231 (1994).

[33] S.A. Ewen and A.M. Soward, Geophys. Astrophys. Fluid Dyn. **77**, 263 (1994).

[34] D.R. Fearn, Proc. Roy. Soc. Lond. A. **369**, 227 (1979).

[35] D.R. Fearn, Geophys. Astrophys. Fluid. Dyn. **14**, 102 (1979).

[36] D.R. Fearn, Geophys. Astrophys. Fluid. Dyn. **27**, 137 (1983).

[37] D.R. Fearn, Geophys. Astrophys. Fluid. Dyn. **30**, 227 (1984).

[38] D.R. Fearn, Geophys. Astrophys. Fluid. Dyn. **44**, 55 (1988).

[39] D.R. Fearn, Geophys. Astrophys. Fluid. Dyn. **49**, 173 (1989).

[40] D.R. Fearn and M.R.E. Proctor, J. Fluid. Mech. **128**, 1 (1983).

[41] D.R. Fearn, P.H. Roberts and A.M. Soward, Convection, Stability and the Dynamo in Pitman Research Notes in Mathematics Series, **168**, 60 (1983).

[42] C.C. Finlay and A. Jackson, Science **300**, 2084 (2003).

[43] C.C. Finlay, Ph.D. Thesis, University of Leeds, U.K., 2005.

[44] C.C. Finlay, Alfvén waves, in: *Encyclopedia of Geomagnetism and Paleomagnetism*, edited by D. Gubbins and E. Herraro-Bervera, 2007, p. 3.

[45] C.C. Finlay, Magnetohydrodynamic waves, in: *Encyclopedia of Geomagnetism and Paleomagnetism*, edited by D. Gubbins and E. Herraro-Bervera, 2007, p. 632.

[46] D. Fultz, J. Meteorology **16**, 199 (1959).

[47] D. Fultz, *Rotating Flows: National Committee for Fluid Mechanics Films*, http://web.mit.edu/fluids/www/Shapiro/ncfmf.html, 1969.

[48] N. Gillet, D. Brito, D. Jault and H.-C. Nataf J. Fluid Mech. **580**, 123 (2007).

[49] H.P. Greenspan, *The Theory of Rotating Fluids*, Cambridge University Press, 1968.

[50] D. Gubbins and P.H. Roberts, Geomagnetism, ed. J.A. Jacobs **2**, 1 (1987).

[51] J. Hayvaerts and E.R. Priest, Astron. Astrophys. **117**, 220 (1983).

[52] R. Hide, Philos. Trans. Roy. Soc. Lond. A. **259**, 155 (1966).

[53] R. Hide and K. Stewartson, Rev. Geophys. **10**, 579 (1973).

[54] R. Hollerbach, The core-mantle boundary region, AGU Geodynamical Monograph, **31**, 181 (2003).

[55] C.A. Jones and P.H. Roberts, Geophys. Astrophys. Fluid. Dyn. **93**, 173 (2000).

[56] C.A. Jones, A.M. Soward and A.I. Mussa, J. Fluid Mech. **405**, 157 (2000).

[57] C.A. Jones, A.I. Mussa and S.J. Worland, Proc. Roy. Soc. A. **459**, 773 (2003).

[58] Lord Kelvin, Philosoph. Mag. **10**, 155 (1880).

[59] Lord Kelvin, *Proc. Roy. Inst. 4th March 1881* (see also Collected Papers of Lord Kelvin, Vol. 4. pp. 169) 1881.

[60] D.H. Kelley, S.A. Triana, D.S. Zimmerman, A. Tilgner and D.P. Lathrop, Geophys. Astrophys. Fluid Dyn. **101**, 469 (2007).

[61] R.R. Kerswell, J. Fluid. Mech. **274**, 219 (1994).

[62] L. Lacaze, P. Le Gal, and S. Le Dizés, J. Fluid. Mech. **475**, 1 (2004).

[63] L. Lacaze, P. Le Gal, and S. Le Dizés, Phys. Earth Plan. Int. **151**, 194 (2005).

[64] L. Lacaze, W. Herreman, M. Le Bars, S. Le Dizés and P. Le Gal, Geophys. Astrophys. Fluid Dyn. **100**, 299 (2006).

[65] B. Lehnert, Phys. Rev. **94**, 815 (1953).

[66] B. Lehnert, Astrophys. J. **119**, 647 (1954).

[67] M.J. Lighthill, J. Fluid. Mech. **26**, 411 (1966).

[68] M.J. Lighthill, *Waves in Fluids*, Cambridge University Press, 1978.

[69] S. Lundquist, Phys. Rev. **107**, 1805 (1949).

[70] W.V.R. Malkus, J. Fluid Mech. **28**, 793 (1967).

[71] W.V.R. Malkus, Geophys. Astrophys. Fluid Dyn. **48**, 123 (1989).

[72] A.D. McEwan, J. Fluid Mech. **40**, 603 (1970).

[73] P. Melchoir, *Physics of the Earth's Core*, Pergamon Press, 1986.

[74] H.K. Moffatt, *Magnetic Field Generation in Electrically Conducting Fluids*, Cambridge University Press, 1978.

[75] H.-C. Nataf, T. Alboussiére, D. Brito, P. Cardin, N. Gagniére, D. Jault, J.P. Masson and D. Schmitt, Geophys. Astrophys. Fluid Dyn. **100**, 281 (2006).

[76] E.N. Parker, Astrophys. J. **122**, 293 (1955).

[77] J. Pedlosky, *Geophysical Fluid Dynamics*, Springer-Verlag, New York, 1987.

[78] H. Poincaré, Acta Math. **7**, 259 (1885).

[79] M.R.E. Proctor, *Lectures in Solar and Planetary Dynamos*, edited by M.R.E. Proctor and A.D. Gilbert, 1994, p. 97.

[80] M. Rieutord and L. Valdettaro, J. Fluid Mach. **341**, 77 (1997).

[81] M. Rieutord, B. Georgeot and L. Valdettaro, J. Fluid Mech. **435**, 103 (2001).

[82] P.H. Roberts and A.M. Soward, Ann. Rev. Fluid. Mech. **4**, 117 (1972).

[83] P.H. Roberts and K. Stewartson, Proc. Roy. Soc. Lond. A. **277**, 287 (1974).

[84] P.H. Roberts, Reprinted in Magnetohydrodynamics and Earth's core: Selected works of Paul Roberts, ed. A.M. Soward, Published by Taylor and Francis (2003), **90**, 261 (1977).

[85] P.H. Roberts and D.E. Loper, J. Fluid. Mech. **90**, 641 (1979).

[86] P.H. Roberts and C.A. Jones, Geophys. Astrophys. Fluid. Dyn. **92**, 289 (2000).

[87] B. Roberts, *In Solar System Magnetohydrodynamics*, eds. E.R. Priest and A.W. Hood, Published by Cambridge University Press, 1991, p. 37.

[88] C.-G., Rossby, J. Mar. Res. **2**, 33 (2000).

[89] D.A. Schecter, J.F. Boyd and P.A. Gilman, Astrophys. J. **551**, L185 (2001).

[90] D. Schmitt, T. Alboussiére D. Brito, P. Cardin, N. Gagniére, D. Jault, H.-C. Nataf, J. Fluid Mech. **604**, 175–197 (2008).

[91] B. Seyed-Mahmoud, K. Aldridge and G. Henderson, Phys. Earth Plan. Int. **142**, 257 (2004).

[92] J.A. Shercliff, *Magnetohydrodynamics: National Committee for Fluid Mechanics Films*, http://web.mit.edu/fluids/www/Shapiro/ncfmf.html, 1965.

[93] A.M. Soward, Phys. Earth. Planet. Int. **20**, 134 (1979).

[94] A.M. Soward and E. Dormy, Dynamics of rapidly rotating fluids: Waves and boundary layers, in: *Mathematical Aspects of Natural Dynamos* (Published by Taylor and Francis), 2007, p. 151.

[95] K. Stewartson, Philos. Trans. Roy. Soc. Lond. A. **299**, 173 (1967).

[96] K. Stewartson, in: *Rotating Fluids in Geophysics*, edited by A.M. Soward and P.H. Roberts, (1978), p. 67.

[97] P.A. Sturrock, *Plasma Physics*, Cambridge University Press, 1994.

[98] D.J. Tritton, *Physical Fluid Dynamics*, Oxford University Press, 1987.

[99] M.R. Walker, C.F. Barenghi and C.A. Jones, Geophys. Astrophys. Fluid. Dyn. **8**, 261 (1998).

[100] M.R. Walker and C.F. Barenghi, Phys. Earth. Planet. Int. **111**, 35 (1999).

[101] S.J. Worland, Ph.D. Thesis, University of Exeter, U.K., 2004.

[102] K. Zhang, J. Fluid Mech. **248**, 203 (1993).

[103] K. Zhang, Proc. Roy. Soc. Lond. A. **448**, 245 (1995).

[104] K. Zhang, Phys. Earth. Planet. Int. **111**, 93 (1999).

[105] K. Zhang and X. Liao, J. Fluid Mech. **518**, 319 (2004).

[106] K. Zhang and D. Gubbins, Math. and Comp. Model. **36**, 389 (2002).

[107] K. Zhang and G. Schubert, Ann. Rev. Fluid. Mech. **32**, 409 (2000).

[108] K. Zhang, P. Earnshaw, X. Liao and F.H. Busse, J. Fluid Mech. **437**, 103 (2001).

[109] K. Zhang, X. Liao and P. Earnshaw, J. Fluid Mech. **504**, 1 (2004).

[110] K. Zhang, X. Liao and F.H. Busse, J. Fluid Mech. **575**, 449 (2007).